Available online at www.sciencedirect.com

ScienceDirect

journal homepage: www.elsevier.com/locate/he

Substituted heterocycles as new candidates for liquid organic hydrogen carriers: *In silico* design from DFT calculations

Rodolfo Izquierdo [a,*], *Néstor Cubillan* [b], *Mayamaru Guerra* [c], *Merlín Rosales* [d]

[a] *Laboratorio de Química Teórica y Computacional, Departamento de Química, Facultad Experimental de Ciencias, Universidad Del Zulia, Maracaibo, Venezuela*

[b] *Programa de Química, Facultad de Ciencias Básicas, Universidad Del Atlántico, Barranquilla, Colombia*

[c] *Laboratorio de Óptica y Procesamiento de Imágenes, Facultad de Ciencias Básicas, Universidad Tecnológica de Bolívar, Turbaco, Colombia*

[d] *Laboratorio de Química Inorgánica, Departamento de Química, Facultad Experimental de Ciencias, Universidad Del Zulia, Maracaibo, Venezuela*

HIGHLIGHTS

- DFT calculations for hydrogenation/dehydrogenation of heterocycles was examined.
- Thermodynamic calculations with M06HF are consistent with those of the G3(MP2) one.
- The thermodynamic parameters for reactions of *N*- and *S*-heterocycles are discussed.
- Pyrrole and thiophene could be key structures for the development of new LOHCs.
- It is the first report on the potentiality of allyl- and thienyl-pyrrole as LOHCs.

GRAPHICAL ABSTRACT

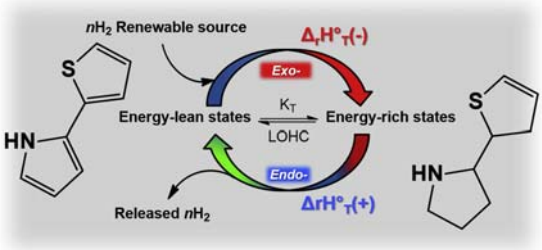

ARTICLE INFO

Article history:
Received 15 December 2020
Received in revised form
6 February 2021
Accepted 24 February 2021
Available online xxx

ABSTRACT

A new set of compounds based on *N*- and *S*-heterocycles were investigated through Density Functional Theory (DFT) for their use as liquid organic hydrogen carriers (LOHCs). The hydrogenated forms of these compounds could release hydrogen within the most important technical requirements in mobile and stationary applications. In this work, the potential of the 1*H*-pyrrole/tetrahydro-1*H*-pyrrole and thiophene/tetrahydrothiophene pairs as possible leader structures to synthesize more sustainable LOHCs from costless oil-refining and oil-hydrotreating by-products is shown. According to DFT-M06-HF results,

* *Corresponding author.*
E-mail address: reis131182@gmail.com (R. Izquierdo).

https://doi.org/10.1016/j.ijhydene.2021.02.201

Please cite this article as: Izquierdo R et al., Substituted heterocycles as new candidates for liquid organic hydrogen carriers: *In silico* design from DFT calculations, International Journal of Hydrogen Energy, https://doi.org/10.1016/j.ijhydene.2021.02.201

Keywords:
Liquid Organic hydrogen carriers (LOHCs)
Heterocycles
Pyrrole
Thiophene
Density functional theory (DFT)
M06-HF

the 3-allyl-1*H*-pyrrole/3-allyl-tetrahydro-1*H*-pyrrole pair presented an adequate theoretical hydrogen storage capacity (3.6 %wt H) and a high theoretical dehydrogenation equilibrium yields (% ε_d = 67.8%) at 453 K. Therefore, this pair is recommended for hydrogen storage stationary applications. On the other hand, the 2-(thiophen-2-yl)-1*H*-pyrrole/2-(2,3-dihydrothiophen-2-yl)tetrahydropyrrole pair proved to be suitable for both mobile and stationary applications; the storage capacity of this pair was 3.9 %wt H and the theoretical dehydrogenation equilibrium yields at 453 K (% ε_d = 28.1%) was considered moderate.

Introduction

In the continuing transition to use renewable energy, the intermittent energy sources (solar and wind power) will need new methods to store and transport energy in order to balance the world supply and demand [1,2]. Hydrogen is widely considered an ideal energy carrier from the sustainability point of view due to the following reasons: (**i**) ideally, it could be produced entirely from renewable energy sources [3,4], (**ii**) the hydrogen energy cycle is based on non-toxic species interconversion: water, oxygen, and hydrogen [5–7] and (**iii**) molecular hydrogen is the lightest molecule (molecular weight (MW) = 2.016) with the highest known energy content ($\Delta_r H^{\circ}_{298.15K} = -241.8$ kJ mol^{-1}, reaction 1) [2,8].

$$H_2 + O_2 \rightarrow H_2O \quad (1)$$

In this sense, energy suppliers need different storage technologies. Currently, hydrogen storage technologies (HSTs) are identified as a key challenge and the largest barrier towards the hydrogen economy [8–15]. HSTs include both physical (compression/liquefaction) and chemical storages [16]. Among the chemical storage technologies, the liquid organic hydrogen carriers (LOHCs) are highlighted by loading and unloading considerable amounts of hydrogen (H_2) in a sustainable cyclical process (Scheme 1). The LOHCs are liquids or solids of low melting point that can be reversibly hydrogenated and dehydrogenated under moderate reaction conditions in presence of a catalyst [17–19].

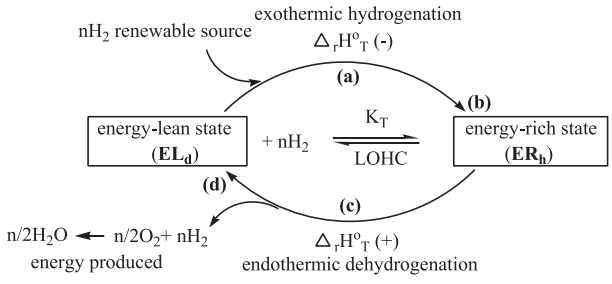

Scheme 1 – Illustration of the LOHC concept according to Aakko-Saksa et al. [22]: (a) LOHC is hydrogenated to a state ER_h, (b) hydrogenated LOHC is transported to end-user (c) H_2 is released and used as useful energy (d) LOHC is dehydrogenated to a state EL_d and dehydrogenated form is transported to the hydrogenation site.

The LOHCs basic theory indicates that these substances can be found in two chemical states. The first is an energy-rich state (ER_h), in which a LOHC stores **2n** hydrogen atoms (where **n** is an integer number) through an exothermic reaction. The second state corresponds to an energy-lean state (EL_d) where the hydrogen-loaded LOHC releases **n** H_2 molecules through an endothermic reaction. Subsequently, the hydrogen produced by ER_h-EL_d interchange is used for energy production, and the LOHC is regenerated [20–22].

The LOHCs can be easily integrated to applications with portable power (on-board), stationary power (off-board), and energy transportation [18,21,23,24]. According to Müller et al. [25], the LOHCs must meet six ideal requirements in order to be used in the hydrogen distribution alongside the development for on-board applications [25]: (**i**) non-toxicity, the acceptable toxicity limit is the octane lethal dose ($LD_{50rat,oral}$ = 1297 mg kg^{-1}) [17], (**ii**) easiness to handle solid or liquid with low vapor pressure (below 0.1 bar), (**iii**) low prices or desirably obtained from by-products or residues of industrial chemical processes (ecofriendly LOHCs) [26], (**iv**) high gravimetric storage density, which is conventionally measured in theoretical [4,27,28] and experimental [29,30] investigations from the theoretical hydrogen weight percentage (% wt H) for completed hydrogenation reaction of EL_d to ER_h, (substances with % wt H superior to 5.5 are considered efficient hydrogen container [31]; however, currently, a lower minimum storage capacity of 4.5% wt H has been established special on-board applications [32]), (**v**) thermally stable substance, i.e. low melting points (mp < 273 K) and high boiling points (bp), and (**vi**) hydrogenation as well as dehydrogenation can be performed at reasonable technical conditions; hydrogenation reaction must be selective, meanwhile dehydrogenation reaction must occur easily and reversibly. The main strategy to achieve this goal is based on reducing the temperature of dehydrogenation by modification of the LOHC molecule to reduce the enthalpy of the reaction [11]. One starting point for modeling hydrogen storage consists of carrying out the theoretical equilibrium calculations at 453 K. Jessop et al. [33] suggested that this temperature should be limited for operating conditions onboard a fuel cell vehicle and stationary applications such as stand-alone energy systems, back-up systems [17].

Finally, in addition to these requirements, a seventh aspect should be included: there must be at least one efficient catalyst for the hydrogenation/dehydrogenation of the EL_d/ER_h pair [18,34]. In fact, several researchers have studied the possibility to use catalytic systems for the reversible

hydrogenation/dehydrogenation reactions employing organic hydrogen carriers. Recently, Shimbayashi and Fujita [18] reviewed a series of works on the use of catalysts for this purpose, which are promising to application to hydrogen storage.

There are different materials commonly considered as LOHCs or pairs EL_d/ER_h. Initially oil-derivatives cyclic hydrocarbons were the simplest candidates. Two emblematic examples are the pairs toluene/methylcyclohexane [35] and dibenzyltoluene/perhydrodibenzyltoluene [36], which presented stationary and energy transport applications with high technology readiness levels (TRL) [37]. Despite their applications, these compounds are expensive industrial commodities with several toxicity concerns, and a relationship with occupational cancer-like diseases [38]. Consequently, new LOHCs environmentally friendly and less toxic are justified [39]. Recently, Verevkin et al. [40] reported a theoretical-experimental study using furfuryl alcohol as a potential LOHC. Despite the efforts in sustainability, their results showed that this compound was not viable as a LOHC because of its low calculated enthalpies (-77.1 kJ mol^{-1}) and storage capacities (2.9 % wt H). Tang et al. [41] published the first *ab-initio* theoretical study for a potential natural LOHC (trisphaeridine/perhydrotrisphaeridine) based on the extraction of trisphaeridine from the *Amaryllidaceae* alkaloids. Despite the low dehydrogenation enthalpy and hydrogen storage capacity, the use of large amounts of expensive solvents, sophisticated separation methods and complex syntheses limited its application [42]. According to what has been published so far, everything seems to indicate that the use of natural LOHCs is not a viable alternative now.

A reasonable alternative to natural LOHCs is based on heterocyclic compounds. This strategy was first introduced by Pez et al. [43]. The calculations suggested that by replacing carbon atoms in polycyclic aromatic hydrocarbons by nitrogen atoms, the endothermic and endergonic character of the dehydrogenation process decreases. This implies a feasibility of the reaction under mild conditions, much better than the cyclic hydrocarbons. These conclusions were independently corroborated by Crabtree et al. [20,44] and Müller et al. [25]. Besides changing the thermodynamic driving force of the dehydrogenation process, the presence of heteroatoms within a cyclic hydrocarbon can produce a positive effect on the activities when using both homogeneous and heterogeneous catalysts for the dehydrogenation process, which is the challenge in the LOHCs [19,45,46]. The LOHCs based on X-heterocyclic compounds (X = N and S) has advantages to consider. For example, according to the U.S. Food and Drug Administration (FDA), *N*- and *S*-heterocycles occupy an important place as raw materials for drug development [47,48], therefore their toxicities must be manageable. Additionally, *N*- and *S*-heterocycles are by-products from oil-refining [49,50] and this fact represents a challenge for hydrotreating [51]. Consequently, from the green chemistry perspective, the use of by-products as LOHCs are economically attractive and sustainable [52]. Among the *N*-heterocycles compounds previously studied, the following EL_d/ER_h pairs can be featured: 1-phenylpyrazole/tetrahydropyrazole [53], 4-aminopyridine/4-aminopiperidine [33], quinoline/1,2,3,4-tetrahydroquinoline [34], indole/2,3-dihydroindole [54], 1,2-dimethylindole/1,2-dimethyloctahydroindole [30], carbazole/perhydrocarbazole [22] and *N*-ethylcarbazole/*N*-ethylperhydrocarbazole [55]. On the other hand, the EL_d/ER_h pairs based on *S*-heterocycles have been scarcely studied both theoretical and experimentally. Only the 2-methylthiophene/2-pentanethiol pair was proposed as LOHC by Zhao et al. [31], while Müller et al. [25] theoretically studied the thiophene/tetrahydrothiophene pair as a LOHC candidate.

Taking into consideration the above-mentioned evidences, in the present paper we report a DFT theoretical study of a series of alkyl substituted *N*- and *S*-heterocycles as new candidates for more sustainable and low-cost LOHCs.

Calculation procedures

The reaction of thiophene and 2-acetyl-pyrrole to give 2-acetyl-thiophene and pyrrole (reaction 2) was used to select the best functional capable of reproducing the $\Delta_r H^\circ_T$ calculated with G3(MP2) method. G3(MP2) calculations were used as a standard gold, due to their accurate thermochemistry parameters and the performance in estimating formation heats ($\Delta_f H^\circ_T$) for heteroatom aromatic rings [56].

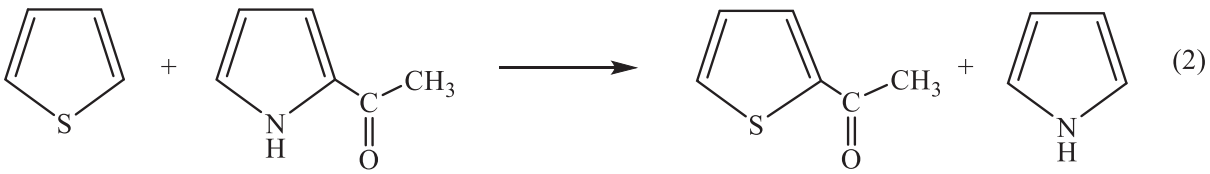

(2)

All calculations were performed with the Gaussian-2016 (G16) [57] computational package and using Density Functional Theory (DFT) framework. Several functionals according to the Truhlar et al. [58,59] classification were tested: (**i**) generalized gradient approximation functionals (GGAs), PBEPBE; (**ii**) meta-GGA functionals (M-GGAs), M06-L, SOGGA11, M11-L; (**iii**) no separable gradient approximation functionals (NGAs), N12; (**iv**) meta-NGA functionals (M-NGAs), MN12-L, MN15-L; (**v**) global hybrid-GGA functionals (H-GGA,G), O3LYP, X3LYP, B3LYP, B3LYP-D3 and SOGGA11-X; (**vi**) global hybrid-M-GGA functionals (H-M-GGA,G), PW6B95, PW6B95D3, M06, M06−2X, M06-HF; (**vii**) hybrid-range-separated functionals (H,RSs), M11, ωB97X and ωB97X-D; (**viii**) hybrid-screened-exchange functionals (H,SXs), N12-SX and MN12-SX.

Please cite this article as: Izquierdo R et al., Substituted heterocycles as new candidates for liquid organic hydrogen carriers: *In silico* design from DFT calculations, International Journal of Hydrogen Energy, https://doi.org/10.1016/j.ijhydene.2021.02.201

Functionals B3LYP-D3, PW6B95D3 and ωB97X-D include an empirical dispersion correction (-D). From (**i**) to (***iv***) are pure (P) or local functionals, and from (***v***) to (***vii***) are hybrids or nonlocal (H) functionals. The 6-31G(d), 6−311++G(3df,3pd), aug-cc-pVDZ and aug-cc-pVTZ basis sets were used.

The geometries were fully optimized, and their vibrational frequencies were obtained to verify the absence of negative eigenvalues in the hessian matrix. All calculations of the reaction thermodynamic functions, $\Delta_r H^\circ_T$ (enthalpy) and $\Delta_r G^\circ_T$ (free energy) for either the reaction used for validation or the hydrogenation of the heterocyclic ring molecule were performed at 1 bar and temperature range 298−453 K.

Schemes 2 and 3 show the simple heterocycle compounds and fused ones, respectively, which were used in the present work. The following notation will be used.

(i) Fully dehydrogenated heterocyclic molecules were denoted by the first or the first two letters (some few cases by the first three or four ones) of the name: for example, thiophene and pyridine (C_9H_7N) are labeled as **T** and **Py**, respectively.

(ii) Molecules with a complex name, such as benzo[*b*]thiophene and 4*H*-tiopyrane, were denoted combining the labels of each fragment (**BT** and 4*H*-**TPyr**).

(iii) The substituents on the heterocyclic ring are labeled as Me (methyl), Et (ethyl), Pr (propyl) indicating the number corresponding to the position of substitution.

(iv) Partial or fully hydrogenated heterocyclic molecules were denoted with the first letter of the prefix indicating the number of hydrogen atom added preceded by the numbers of the carbon atoms where the hydrogen atoms were added plus the word "hydro" before the name of the heterocyclic compound. For example, 1,2-dihydropyridine and 1,2,3,4-tetrahydro pyridine were denoted as 1,2-**DHPy** and **1,2,3,4-THPy**, respectively; the fully hydrogenated **Py** is denoted as **Pip** (piperidine).

All experimental properties, such as melting (mp) and boiling (bp) points, and LD_{50}, were obtained from the Sigma-Aldrich technical manual [60] and Chemspider website [61]. In the case of existing substances without experimental measurements, the values were calculated using the ACD/Labs prediction model found at the ChemSpider website (procedure 1, p1) [61]. Finally, for non-existing or non-synthesized compounds, these values were calculated with the EPA compTox predictor model found at the EPA website (procedure 2, p2) [62].

Table 1 − $\Delta_r H°298K$ signed (E_r) and unsigned relative (%E_r) errors for the reaction of thiophene and 2-acetyl-pyrrole to generate 2-acetyl-thiophene and pyrrole.

Pure Functional	Type	$\Delta_r H°298K$ (kJ mol^{-1})	E_r (kJ mol^{-1})[a]	%E_r[b]		
PBEPBE	P-GGA	23.7/23.0[c]	-5.3/-4.6[c]	28.8/25.0[c]		
M06-L	P-M-GGA,P	24.7/22.9	-6.3/-4.5	34.2/24.5		
SOGGA11	P-M-GGA,P	23.4/22.6	-5.0/-4.2	27.2/22.8		
M11-L	P-M-GGA,P	22.2/28.1	3.8/-9.7	20.7/52.7		
MN12-L	P-M-NGA, P	24.0/23.0	-5.6/-4.6	30.4/25.0		
N12	P-NGA, P	27.7/24.3	-9.3/-4.9	50.5/32.1		
MN15-L	P-M-NGA,P	23.4/22.8	-5.0/-4.4	27.1/23.9		
Hybrid Functional	**Type**	**$\Delta_r H°298K$ (kJ mol^{-1})**	**E_r (kJ mol^{-1})**	**%E_r**	**X[d]**	**ω[e]**
O3LYP	H-GGA, G	24.3/23.7	-5.9/-5.3	31.9/29.0	11.61	-
X3LYP	H-GGA, G	23.7/22.8	-5.3/-4.4	28.8/24.0	21.8	
B3LYP	H-GGA, G	23.7/22.8	-5.3/-4.4	28.8/23.9	21.98	-
B3LYP-D3	H-GGA, GD3,G	22.0/21.0	-3.6/-2.6	19.6/14.1		
PW6B95	H-M-GGA, G	22.9/22.1	-4.5/-3.7	24.5/20.1	28	-
PW6B95D3	H-M-GGA, GD3,G	22.1/21.4	-3.7/-3.0	20.1/16.3	46	-
M06	H-M-GGA, G	22.5/21.4	-4.1/-3.0	22.3/16.3	27	-
SOGGA11-X	H-GGA,G	23.1/22.7	-4.7/-4.3	25.5/23.4	40.15	-
M06-2X	H-M-GGA, G	21.3/20.7	-2.9/-2.3	15.8/12.5	54	-
M06-HF	H-M-GGA, G	19.3/19.1	-0.9/-0.7	4.9/3.8	100	-
M11	H-M-GGA, RS	22.4/17.4	-4.0/1.0	21.7/5.4	42.8/100	0.25
ωB97X	H-GGA,RS	22.3/21.5	-3.9/-3.1	21.2/16.8	15.77/100	0.3
ωB97X-D	H-GGA, GD3,RS	23.4/22.5	-5.0/-4.1	27.1/22.3	22.2/100	0.2
N12-SX	H-NGA,SX	24.4/23.6	-6.0/-5.2	32.6/28.3	25/0	0.11
MN12-SX	H-NGA,SX	22.2/21.5	-3.8/-3.1	20.6/16.8	25/0	0.11
ab-initio	Type	$\Delta_r H°298K$ (kJ mol^{-1})	E_r (kJ mol^{-1})	%E_r		
HF	-	23.3/22.3	-4.9/-3.9	26.6/21.2		
MP2	-	19.3/18.8	-0.9/-0.4	4.9/2.7		

[a] G3(MP2) reference value [56], ($\Delta_r H^\circ_{298.15K}$ [56] = 18.4 kJ mol-1), Er = 18.4 kJ mol^{-1}-$\Delta_r H^\circ_{298.15K}$.

[b] $\%E_r = \left|\frac{E_r}{18.4\ \text{kJ mol}^{-1}}\right| x\ 100$

[c] 6−311++G(3df,3pd) values/6-31G(d) values.

[d] HF Exchange (%) or 100-X of local exchange.

[e] ω is the optimal value for the RS (borh^{-1}).

Please cite this article as: Izquierdo R et al., Substituted heterocycles as new candidates for liquid organic hydrogen carriers: *In silico* design from DFT calculations, International Journal of Hydrogen Energy, https://doi.org/10.1016/j.ijhydene.2021.02.201

Results and discussion

This work is comprised by three sections: (i) a methodology validation by the calculation of reaction thermodynamics functions to select the best functional by reproducing the $\Delta_r H^\circ_T$ calculated with G3(MP2), (ii) the calculations of thermodynamic functions for the hydrogenation of some heteroatom ring molecules and their comparison with non-heteroatom ring molecules, and (iii) the virtual screening by structural modifications of some pairs to achieve efficient LOHC's according to the ideal requirements proposed by Müller et al. [25].

$\Delta_r H^\circ_{298K}$ calculation for the reaction of thiophene and 2-acetyl-pyrrole to 2-acetyl-thiophene and pyrrole.

Table 1 summarizes the results for the reaction 2. In the top of the table the results produced with the pure functionals are presented, in the middle section the results with the hybrid functionals and the results at *ab-initio* level are shown in the bottom. Generally, due to the increasing size of the basis set from 6 - 31G(d) to 6−31++G(3df,3pd), the magnitude of the calculated $\Delta_r H^\circ_T$ and the signed error, E_r, values for pure functional decreases, whereas for H-GGA and H-M-GGA the increasing basis set decreases E_r values.

For the pure functionals, the conceptually correct GGA functional (PBEPBE) and the more-sophisticated M-GGA Minnesota functionals, except M11-L, overestimate the reference value (see E_r in Table 1). All pure functionals produce $\Delta_r H^\circ_{298K}$ values with unsigned relative errors ($\%E_r$) higher than 5%. Therefore, we do not recommend these pure functionals to calculate $\Delta_r H^\circ_T$ for similar reactions studied in this section.

The calculated $\Delta_r H^\circ_T$ are higher than the reference value ($E_r < 0$ kJ mol^{-1}) for both H-GGA and H-M-GGA global hybrid functionals. Conversely to Zhao and Truhlar [63], PW6B95 and PW6B95D3 functionals gave no better results for thermochemical calculations. The signed error has a linear relationship with the HF Exchange (%, X) of the global hybrid functionals, as shown in Fig. 1. This plot reveals a decreasing unsigned error whereas increasing HF exchange described by the equation: $\%E_r = -0.300X + 34.226$ ($p < 2.50 \times 10^{-5}$, $r^2 = 0.93$). Similar results were found for the 6−31++G(3df,3pd), aug-cc-PVDZ and aug-cc-PVTZ basis sets (see Fig. 1).

The HF exchange contribution in the global hybrid functionals is essential for $\Delta_r H^\circ_{298K}$ calculation. The M06-HF functional (X = 100) could reproduce the reference $\Delta_r H^\circ_{298K}$ value, $\%E_r < 5\%$. A good performance of this functional was also found for reaction energies calculation of DARC14 database, 14 typical Diels-Alder reactions ($E_r = -7.1$ kJ mol^{-1}) [58].

Although the functional M06-HF produces the best $\Delta_r H^\circ_{298}$ values for reaction 2, $\%E_r$ values between 3.8% and 4.9% were obtained. It would be expected that ascending on the Jacob's ladder result in a better accuracy. This is supported by several benchmark calculations to test the functionals against some reaction energies databases [58,64–67]. Conversely, $\%E_r$ results suggest that the RS functionals (M11, ωB97X and ωB97X-D), as well as the more sophisticated SX functionals (N12-SX and MN12-SX), do not improve the $\Delta_r H^\circ_{298K}$ calculated against the referenced value.

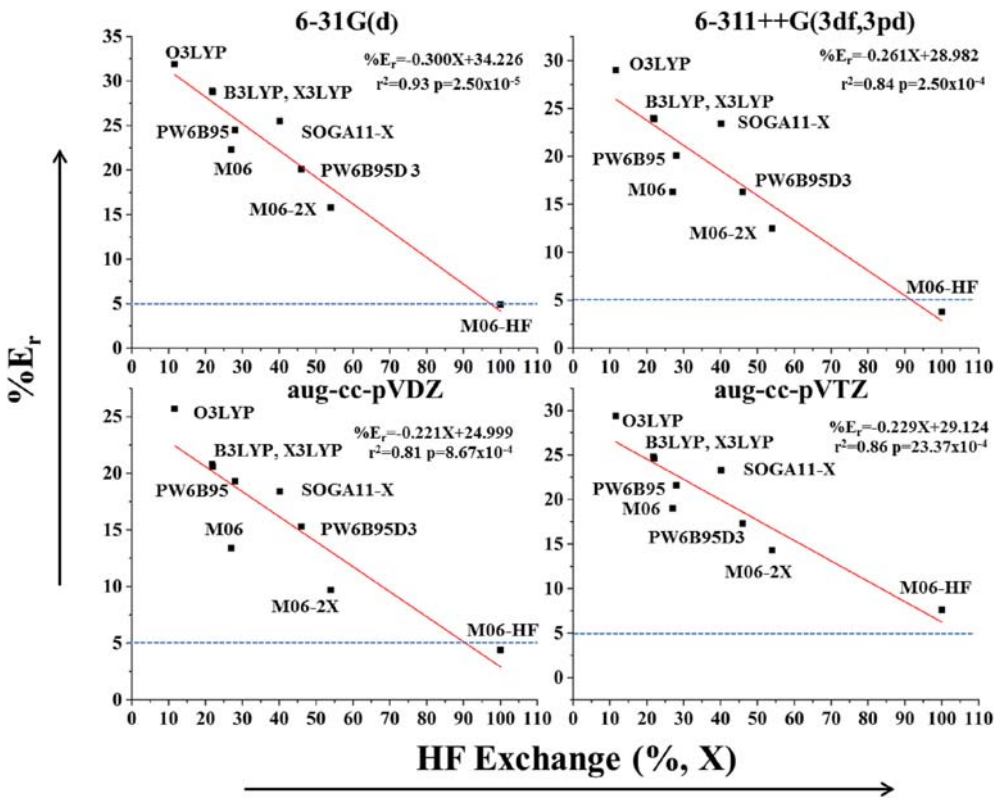

Fig. 1 − Plot HF Exchange (%,X) vs $\%E_r$ for the global hybrid functionals with the basis set: 6-31G(d), 6−311++G(3df,3pd), aug-cc-pVDZ and aug-cc-pVTZ.

Please cite this article as: Izquierdo R et al., Substituted heterocycles as new candidates for liquid organic hydrogen carriers: *In silico* design from DFT calculations, International Journal of Hydrogen Energy, https://doi.org/10.1016/j.ijhydene.2021.02.201

The inclusion of the Grimme's dispersion in the functionals B3LYP, PW6B95 and ωB97X did not reduce the E_r and % E_r values (see Table 1). At the DFT level, M06-HF/6−311++G(3df,3pd) and M06-HF/6-31G(d) combinations produced the best $\Delta_rH^\circ_T$ values with %E_r of 3.8% and 4.9%, respectively. Therefore, the M06-HF functional presented a similar performance to that of MP2 in calculating $\Delta_rH^\circ_{298K}$ for reaction 2 (see Table 1). Since reaction 2 involves rupture and formation of the bonds in thiophene and pyrrole molecules, the M06-HF/6−311++G(3df,3pd) and M06-HF/6-31G(d) combinations are expected to produce good enthalpy values for the hydrogenation/dehydrogenation reactions of heteroatom aromatic ring molecules. The results of the following sections were calculated with the M06-HF/6-31G(d) combination.

Calculations of thermodynamic functions for the hydrogenation of heterocycle rings of some molecules

In this section, the thermodynamic functions for the hydrogenation of heteroaromatic molecules were calculated; the thermodynamic values for the hydrogenation of the analogue non-heteroatom ring molecules are included in Supplementary Material I (SM-I) for comparison. The goal was to find the best reversible hydrogenation reactions to store **2n** hydrogen atoms from a thermodynamic point of view in the proposed heterocycles. To achieve this objective, it must be clarified that the free energy of reaction, $\Delta_rG^\circ_T$, as the thermodynamic driving force of the chemical reaction at a given temperature, can be calculated from the enthalpy of reaction ($\Delta_rH^\circ_T$), and the entropy of reaction ($\Delta_rS^\circ_T$), according to equation (3).

$$\Delta_rG^\circ_T = \Delta_rH^\circ_T - T\Delta_rS^\circ_T \quad (3)$$

In Table 2 the hydrogenation reactions involving the compounds of Schemes 3 and 4 are presented. At 298K, almost all hydrogenations were favored by the reaction equilibrium ($|\Delta_rH^\circ_{298K}| > |T\Delta_rS^\circ_{298K}|$). The exception was observed in pyrrole (**Pyrr**), benzene (see MS-I) and quinoline bicycle (**Q**). Although the first hydrogenation reaction of **Pyrr** was exothermic ($\Delta_rH^\circ_{298K} = -10.5$ kJ mol^{-1}), the $T\Delta_rS^\circ_{298K}$ term (33.5 kJ mol^{-1}) dominated over $\Delta_rG^\circ_{298K}$ value. At 298K the reaction was endergonic (see reaction 4). A similar behavior was verified in the hydrogenation reaction of **Q** to 1,2-dihydroquinoline (1,2-**DHQ**, see reaction 32) and reaction of benzene to 1,3-cyclohexadiene (see SM-I). The main cause of this behavior was the highest aromatic stabilization energy (ASE) in the **Pyrr**, **Q** and benzene structures.

The $\Delta_rH^\circ_{298K}$and $\Delta_rG^\circ_{298K}$ values depend on the size and heteroatom nature of the heterocyclic compounds. In molecules with N and S atoms in the cyclic skeleton, a decrease in the exothermicity and exergonicity of the hydrogenation reactions was found.

For the five-atom monocyclic compounds, the isolobal replacement in cyclopentadiene/cyclopentane of one CH/CH_2 fragment by NH/NH in **Pyrr/THPyrr** increased $\Delta_rH^\circ_{298K}$ and $\Delta_rG^\circ_{298K}$ values for total hydrogenation reactions in 115.8 kJ mol^{-1} and 114.0 kJ mol^{-1}, respectively (see reaction 6 in

Table 2 – Thermodynamic functions (kJ mol^{-1}) for the hydrogenation of heteroatom aromatic ring of some molecules calculated from M06-HF/6−31(d) at 298 K and 1 bar.

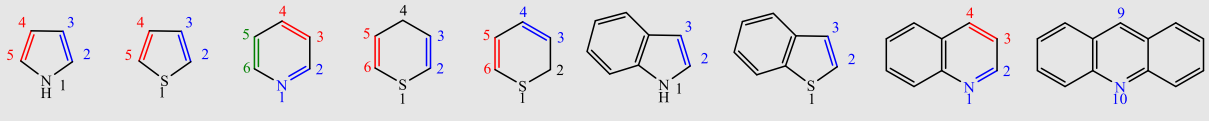

Pyrrole (**Pyrr**) · Thiophene (**T**) · Pyridine (**Py**) · 4*H*-Thiopyran (**4H-Tpy**) · 2*H*-Thiopyran (**2H-Tpy**) · Indole (**In**) · Benzohiophene (**BT**) · Quinoline (**Q**) · Acridine (**A**)

N	Reaction	$\Delta_rH^\circ_T$	$\Delta_rG^\circ_T$	N	Reaction	$\Delta_rH^\circ_T$	$\Delta_rG^\circ_T$
(4)	**Pyrr** + H_2 → 2,3-**DHPyrr**	−10.5	23.0	(22)	**Py** + $3H_2$ → **Pip**	−220.2	−112.4
(5)	2,3-**DHPyrr** + H_2 → **THPyrr**	−114.8	−82.0	(23)	4H-**TPyr** + H_2 → 3,4-**DH**-2H-**TPyr**	−133.6	−96.7
(6)	**Pyrr** + $2H_2$ → **THPyrr**	−125.4	−59.0	(24)	3,4-**DH**-2H-**TPyr** + H_2 →**TH**-2H-**TPyr**	−133.4	−95.7
(7)	**T** + H_2 → 2,3-**DHT**	−56.0	−23.6	(25)	2H-**TPyr** + H_2 → 3,4-**DH**-2H-**TPyr**	−127.9	−91.6
(8)	2,3-**DHT** + H_2 → **THT**	−134.7	−98.7	(26)	2H-**TPyr** + H_2 → 3,6-**DH**-2H-**TPyr**	−121.2	−85.1
(9)	**T** + $2H_2$ → **THT**	−191.3	−122.4	(27)	3,6-**DH**-2H-**TPyr** + H_2 → **TH**-2H-**TPyr**	−140.1	−102.1
(10)	**Py** + H_2 → 2,3-**DHPy**	21.8	54.3	(28)	2H-**TPyr** + **2** H_2 → **TH**-2H-**TPyr**	−267.0	−192.4
(11)	**Py** + H_2 → 3,4-**DHPy**	8.4	41.2	(29)	4H-**TPyr** + **2** H_2 → **TH**-2H-**TPyr**	−261.2	−187.3
(12)	2,3-**DHPy** + H_2 → 2,3,4,5-**THPy**	−125.8	−88.9	(30)	**In** + H_2 → 2,3-**DHIn**	−49.9	−13.3
(13)	2,3-**DHPy** + H_2 → 1,2,3,6-**THPy**	−102.9	−63.3	(31)	**BT** + H_2 → 2,3-**DHBT**	−84.8	−49.5
(14)	3,4-**DHPy** + H_2 → 2,3,4,5-**THPy**	−112.4	−76.2	(32)	**Q** + H_2 → **1,2-DHQ**	−22.1	12.2
(15)	3,4-**DHPy** + H_2 → 2,3,4,5-**THPy**	−124.9	−88.5	(33)	**Q** + H_2 → 1,4-**DHQ**	−36.4	−3.3
(16)	2,3,4,5-**DHPy** + H_2 → **Pip**[a]	−116.2	−77.8	(34)	**Q** + H_2 → 3,4-**DHQ**	−43.2	−7.8
(17)	1,2,3,6-**THPy** + H_2 → **Pip**	−139.1	−101.4	(35)	1,2-**DHQ** + H_2 → 1,2,3,4-**THQ**	−125.8	−88.9
(18)	1,4,5,6-**DHPy** + H_2 → **Pip**	−103.7	−65.6	(36)	1,4-**DHQ** + H_2 → 1,2,3,4-**THQ**	−111.5	−73.3
(19)	**Py** + $2H_2$ → 2,3,4,5-**THPy**	−104.0	−34.6	(37)	3,4-**DHQ** + H_2 → 1,2,3,4-**THQ**	−104.7	−68.8
(20)	**Py** + $2H_2$ → 1,2,5,6-**THPy**	−81.1	−11.0	(38)	**Q** + $2H_2$ → 1,2,3,4-**THQ**	−147.9	−76.7
(21)	**Py** + $2H_2$ → 1,4,5,6-**THPy**	−116.5	−46.8	(39)	**A** + H_2 → 9,10-**DHA**	−100.5	−67.5

[a] **Pip** is the fully hydrogenation product of Py.

Please cite this article as: Izquierdo R et al., Substituted heterocycles as new candidates for liquid organic hydrogen carriers: *In silico* design from DFT calculations, International Journal of Hydrogen Energy, https://doi.org/10.1016/j.ijhydene.2021.02.201

Table 2 and SM-I). A similar increase of $\Delta_rH^\circ_{298K}$ and $\Delta_rG^\circ_{298K}$ values for total hydrogenation reaction was verified for S/S substitution to form the thiophene/1,2,3,4-tetrahydrothiophene (**T/THT**) pair (see reaction **9** in Table 2 and SM-I).

Microscopic reversibility establishes that thermodynamically the hydrogenation is as easy as the dehydrogenation is complicated since it has the same $\Delta_rG^\circ_{298K}$ value with a different algebraic sign.

As shown in Table 2, at 298 K, the thermodynamics of the five-atom monocyclic compounds hydrogenation reactions had an enthalpy control. In these cases, Jessop et al. [33] proposed that an optimum hydrogen storage liquid would have a $\Delta_rH^\circ_{298K}$ hydrogenation per mole of H_2 ($\Delta_rH^\circ_{298K}/n$) close to -50 kJ mol^{-1}, so that a reasonable extent of dehydrogenation could be expected in the temperatures range from 298 K to 453 K. The **Pyrr/THPyrr** and **T/THT** pairs presented $\Delta_rH^\circ_{298K}/n$ values of -62.7 kJ mol^{-1} and -95.7 kJ mol^{-1}, respectively. It is clear that the **Pyrr/THPyrr** pair had desirable thermodynamic characteristics for use as hydrogen storage, while the **T/THT** pair was not suitable. On the other hand, the **T**/2,3-**DHT** pair showed the desired thermodynamic behavior with possible applications in hydrogen storage (see reaction 7 of Table 2).

For the six-atom monocyclic compounds, the isolobal replacement in benzene/cyclohexane of one CH/CH_2 fragment by N/NH in pyridine/piperidine (**Py/Pip**) caused an increase in $\Delta_rH^\circ_T$ and $\Delta_rG^\circ_T$ values for total hydrogenation of 23.1 kJ mol^{-1} and 22.0 kJ mol^{-1}, respectively (see reactions 22 in Table 2 and SM-I). This increase in enthalpy values was similar to a decrease in total dehydrogenation enthalpy (~24.2 kJ mol^{-1}, inverse reaction) published by Crabtree et al. [46] using a DFT-B3LYP methodology. As 4*H*-thiopyran (4*H*-**Tpyr**) and 2*H*-thiopyran (2*H*-**Tpyr**) are non-aromatic molecules, the first and second hydrogenation are highly exothermic and exergonic processes at 298 K. Moreover, their total hydrogenation reactions had the lowest values of $\Delta_rH^\circ_T$ and $\Delta_rG^\circ_T$ among the studied compounds. For the six-atom monocyclic compounds, the total hydrogenation can occur by various pathways involving different positional isomers. In particular, reactions from 10 to 22 showed different routes for the total hydrogenation of the pyridine, while the reactions from 23 to 29 showed different routes for the hydrogenation of thiopyran isomers. No relevant changes were observed in $\Delta_rH^\circ_{298K}$ and $\Delta_rG^\circ_{298K}$ values for the different reaction routes. The **Py/Pip**, 4*H*-**TPyr/TH**-2*H*-**TPy** and 2*H*-**TPyr/TH**-2*H*-**TPy** pairs presented $\Delta_rH^\circ_{298K}/n$ values of -73.4 kJ mol^{-1}, -133.5 kJ mol^{-1} and -130.6 kJ mol^{-1}, respectively. According to the results the six-atom heterocyclic rings were not good candidates to be used in hydrogen storage technologies.

The results of hydrogenation reactions of indole (**In**) and benzo[*b*]thiophene (**BT**) proved potential applications in hydrogen storage. The reactions 30 and 31 show the regioselective hydrogenation of **In** to 2,3-dihydroindole (2,3-**DHIn**) and **BT** to 2,3-dihydro-benzo[*b*]thiophene (2,3-**DHBT**). The presence of the N and S atoms in and **BT** produced an increase in $\Delta_rH^\circ_{298K}$ values of 68.0 kJ mol^{-1} and 33.1 kJ mol^{-1} compared to the indene (see SM-I). These results are similar to those reported by Crabtree et al. [46] for the reaction of dehydrogenation. The thermodynamics for the reaction of **BT** (reaction 31) was like the thermodynamics of the hydrogenation reaction of benzofuran to 2,3-dihydrobenzofuran ($\Delta_rH^\circ_{298K} = -77.0$ kJ mol^{-1} and $\Delta_rG^\circ_{298K} = -42.4$ kJ mol^{-1}). Based on the enthalpy values for reaction 31, the **BT**/2,3-**DHBT** pair was not suitable for LOHC applications. Similar results were reported by Crabtree et al. [46] for the benzofuran/2,3-dihydrobenzofuran and **In**/2,3-**DHIn** pairs.

Furthermore, the bicyclic and tricyclic compounds containing an *N*-heteroatom can undergo the regioselective hydrogenation. The results showed no effect on the thermodynamics for the hydrogenation reaction of quinoline (**Q**) and acridine (**A**), in the reactions 38 and 39, when compared to naphthalene and anthracene (see MS-I). At 298.15 K reactions 38 and 39 did not meet the thermodynamic conditions for the manufacture of LOHCs.

«In silico» screening of new pairs EL_d/ER_h as LOHCs candidates

In the previous section it was remarked that the reaction thermodynamics of the EL_d/ER_h pairs **Pyrr/THPyrr**, **T/THT**, **In**/2,3-**DHIn** showed potential for hydrogen storage. Consequently, we performed an «*in silico*» screening of different structural modifications on these compounds with the aim of obtaining the six ideal technical requirements of an efficient LOHC proposed by Müller et al. [25]. The EL_d/ER_h pairs including the EL_d states based on **In** were excluded. The solid state of the **In** (indole, CAS-120-72-9) under normal conditions (mp = 527 K and bp = 325 K) and low hydrogen storage in the **In**/2,3-**DHIn** pair (1.7 %wt H, see reaction 30) limited its applicability as a LOHC.

Substituents on aromatic heterocycles **Pyrr** (pyrrole, CAS-109-97-7) and **T** (thiophene, CAS-110-02-1) were incorporated in this section. Both **Pyrr** (mp = 250 K and bp = 402 K) and **T** (mp = 235 K and bp = 357 K) are chemically stable liquid compounds under normal conditions and the **Pyrr/THPyrr** and **T/THT** pairs have acceptable hydrogen storage of 5.7 %wt H (reaction 5) and 4.6 %wt H, (reaction 9), respectively. Additionally, the EL_d/ER_h pairs including **Pyrr** and **T** are by-products or wastes from hydrotreating of heavy crude and coal (economic and green production) [49,51,68].

On other hand, there are efficient synthesis methods for substitutions on positions 1, 2, and 3 in structures similar to the ones shown in Scheme 2 [69,70]. Moreover, these structural changes can improve the suitability of these compounds as LOHC. The simple substitution in position 1 on **Pyrr** to obtain 1-methylpyrrole (1-Me**Pyrr**, CAS-96-54-8) increased LD_{50} from 137 mg kg^{-1} to 1400 mg kg^{-1}. Similarly, the simple substitution at position 3 on **T** to yield 3-methylthiophene (3-Me**T**, CAS-616-44-4) produced a desirable increase in the bp from 357.15 K to 390.15 K. In summary, despite the limited toxicity data and few studies on the health and environmental impact of the *N*- and *S*-heterocyclic compounds as LOHCs [17], it is expected that substitutions on some key positions could increase the bp and decrease the toxicity in the pairs **Pyrr**/**THPyrr** and **T**/**THT** or **T**/2,3-**DHT**.

The most relevant conclusion in prior section was that at low temperatures (298K) the hydrogenation reactions of **Pyrr** to **THPyrr** (reaction 6, Table 2) and from **T** to **THT** (reaction 9, Table 2) presented moderate values and negatives in the $\Delta_rH^\circ_{298K}$ y $\Delta_rG^\circ_{298K}$. Since the more complicated the hydrogenation, the easier the dehydrogenation (the same $\Delta_rG^\circ_T$ value

Please cite this article as: Izquierdo R et al., Substituted heterocycles as new candidates for liquid organic hydrogen carriers: *In silico* design from DFT calculations, International Journal of Hydrogen Energy, https://doi.org/10.1016/j.ijhydene.2021.02.201

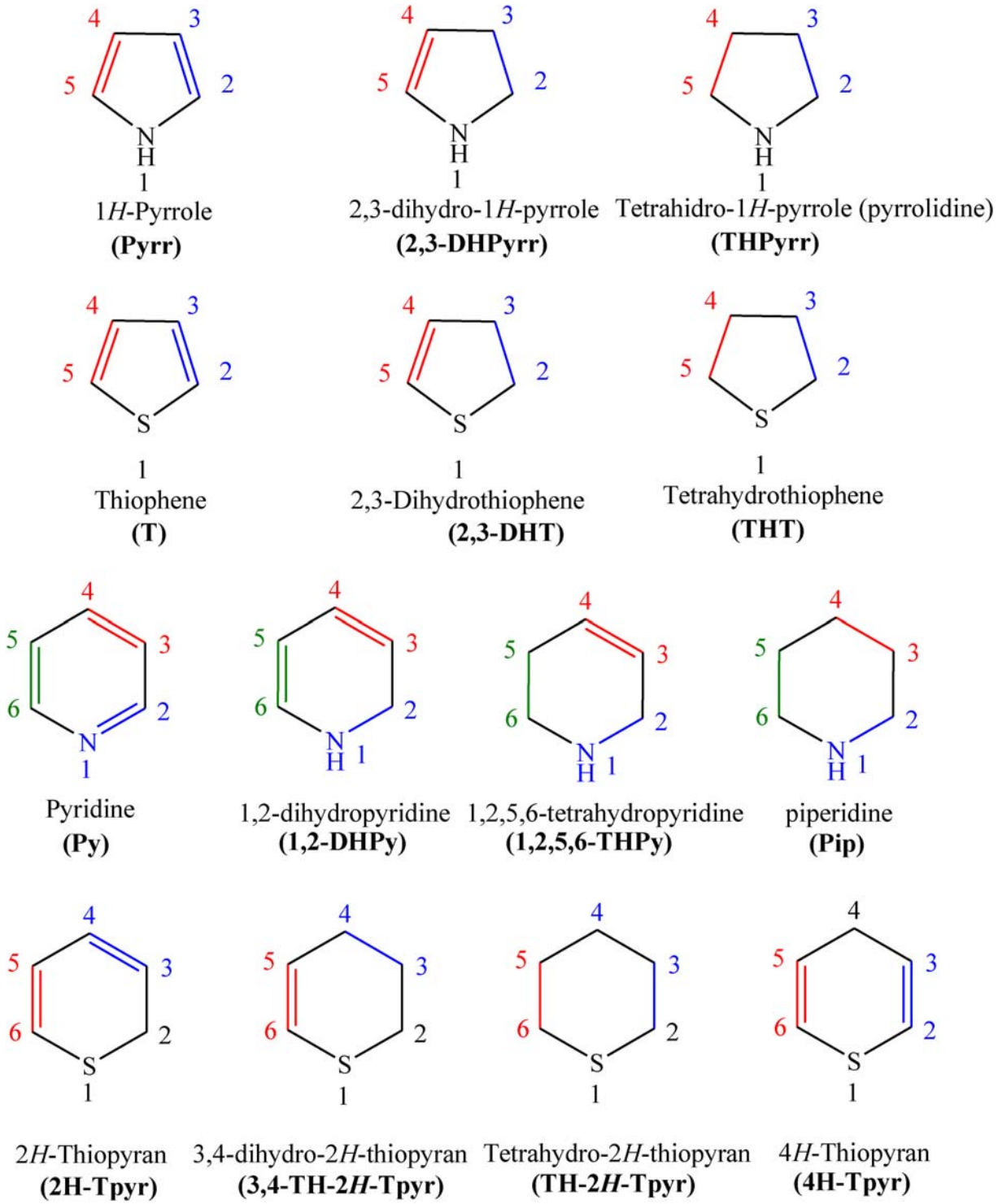

Scheme 2 – Proposed simple five and six atoms heterocycle compounds.

with a different algebraic sign), it is expected that an increase in temperature and substitutions on the **Pyrr** and **T** will improve the hydrogen release in new candidates for LOHCs. Tables 3 and 4 show the $\Delta_r H_T^\circ$ and $\Delta_r G_T^\circ$ calculated at 453 K for hydrogenation reactions involving the substituents on the pyrrole (**Pyrr**) and thiophene (**T**), respectively. The temperature of 453 K is the maximum allowed temperature (T_{max}) for hydrogenation/dehydrogenation in mobile applications for the LOHCs [33]. Since dehydrogenation (hydrogen release) is the most difficult step in LOHCs, the equilibrium constants for the dehydrogenation reaction ($K_d = 1/K_h$) are reported: a K_d close to 1 should facilitate the dehydrogenation. Addtionally, the %wt H were reported to measure the hydrogen storage capacity, while the theoretical dehydrogenation equilibrium yields (%ε_d) calculated from K_d values were incorporated to measure the hydrogen release capacity (values of K_h and K_d

Please cite this article as: Izquierdo R et al., Substituted heterocycles as new candidates for liquid organic hydrogen carriers: *In silico* design from DFT calculations, International Journal of Hydrogen Energy, https://doi.org/10.1016/j.ijhydene.2021.02.201

Table 3 – Thermodynamic functions (kJ mol^{-1}) for the hydrogenation of pyrroles calculated from M06-HF/6–31(d) at 453 K and 1 bar.

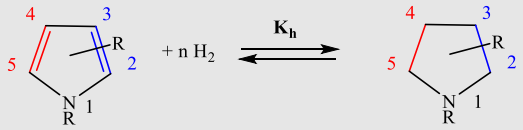

R = H, Me (CH_3), Et (CH_2CH_3), Pr ($CH_2CH_2CH_3$), vinyl ($-HC{=}CH_2$), ethynyl ($-C{\equiv}CH$), allyl ($-CH_2-CH{=}CH_2$)

N	Reagent	bp (K)[a]	n	Product	bp (K)[a]	$\Delta_rG^\circ_T(\Delta_rH^\circ_T)$[b]	K_d[c]	%wt H	% ε_d[d]
(4)	**Pyrr**	403[a1]	1	2,3-**DHPyrr**[e]	393[a2]	41.0 (−13.2)	5.3×10^{4}	2.9	100.0
(5)	**Pyrr**	403[a1]	2	**THPyrr**	361[a1]	−23.1 (−131.4)	2.2×10^{-3}	5.7	7.9
(40)	1-Me**Pyrr**	386[a1]	2	1-Me**THPyrr**	354[a1]	−3.8 (−130.3)	3.6×10^{-1}	4.7	38.3
(41)	2-Me**Pyrr**	371[a1]	2	2-Me**THPyrr**	421[a1]	−15.9 (−133.5)	1.5×10^{-2}	4.7	14.6
(42)	3-Me**Pyrr**	387[a1]	2	3-Me**THPyrr**	373[a2]	−10.0 (−131.6)	7.0×10^{-2}	4.7	23.8
(43)	1-Et**Pyrr**	403[a1]	2	1-Et**THPyrr**	377[a1]	−5.5 (−124.2)	2.3×10^{-1}	4.1	33.8
(44)	2-Et**Pyrr**	464[a1]	2	2-Et**THPyrr**	395[a2]	−3.5 (−123.9)	3.9×10^{-1}	4.1	39.2
(45)	3-Et**Pyrr**	432[a1]	2	3-Et**THPyrr**	395[a2]	−6.9 (−128.3)	1.6×10^{-1}	4.1	30.3
(46)	1-Pr**THPyrr**	419[a2]	2	1-Pr**THPyrr**	405[a2]	−1.9 (−115.8)	6.0×10^{-1}	3.6	43.9
(47)	2-Pr**THPyrr**	453[a2]	2	2-Pr**THPyrr**	423[a2]	−9.2 (−124.3)	8.7×10^{-2}	3.6	25.3
(48)	3-Pr**THPyrr**	453[a2]	2	3-Pr**THPyrr**	432[a2]	−5.1 (−120.5)	2.6×10^{-1}	3.6	34.8
(49)	1-vinyl**Pyrr**	380[a2]	2	1-vinyl**THPyrr**	404[a2]	−17.4 (−138.8)	9.9×10^{-3}	4.1	12.9
(50)	2-vinyl**Pyrr**	463[a2]	2	2-vinyl**THPyrr**	388[a2]	−4.6 (−122.9)	2.9×10^{-1}	4.1	36.1
(51)	3-vinyl**Pyrr**	463[a2]	2	3-vinyl**THPyrr**	400[a2]	−6.1 (−121.4)	2.0×10^{-1}	4.1	32.3
(52)	1-ethynyl**Pyrr**	424[a2]	2	1-ethynyl**THPyrr**	381[a3]	−49.5 (−161.9)	2.0×10^{-6}	4.2	0.8
(53)	2-ethynyl**Pyrr**	465[a2]	2	2-ethynyl**THPyrr**	389[a2]	−8.6 (−119.7)	1.0×10^{-1}	4.2	26.6
(54)	3-ethynyl**Pyrr**	465[a2]	2	3-ethynyl**THPyrr**	389[a2]	−12.0 (−127.1)	4.1×10^{-2}	4.2	20.2
(55)	1-allyl**Pyrr**	420[a2]	2	1-allyl**THPyrr**	398[a2]	−4.6 (−121.8)	2.9×10^{-1}	3.6	36.1
(56)	2-allyl**Pyrr**	453[a2]	2	2-allyl**THPyrr**	415[a2]	−4.6 (−134.0)	2.9×10^{-1}	3.6	36.1
(57)	3-allyl**Pyrr**	453[a2]	2	3-allyl**THPyrr**	425[a2]	5.1 (−118.6)	3.9	3.6	67.8
(58)	1-vinyl**Pyrr**	380[a2]	3	1-Et**THPyrr**	377[a2]	−82.3 (−262.2)	3.3×10^{-10}	6.1	0.2
(59)	2-vinyl**Pyrr**	463[a2]	3	2-Et**THPyrr**	395[a2]	−79.9 (−259.2)	6.2×10^{-10}	6.1	0.3
(60)	3-vinyl**Pyrr**	463[a2]	3	3-Et**THPyrr**	395[a2]	−80.5 (−260.1)	5.3×10^{-10}	6.1	0.3
(61)	1-allyl**Pyrr**	420[a2]	3	1-Pr**THPyr**[b]	05[a2]	−90.3 (−[c]1.6)	3.9×10^{-11}	5.3	0.1
(62)	2-allyl**Pyrr**	453[a2]	3	2-Pr**THPyrr**	423[a2]	−97.2 (−270.8)	6.2×10^{-12}	5.3	0.1
(63)	3-allyl**Pyrr**	453[a2]	3	3-Pr**THPyrr**	432 [a2]	−91.6 (−265.0)	2.8×10^{-11}	5.3	0.1

[a] Boiling point.
[a1] Experimental.
[a2] Theoretical procedure p1 and.
[a3] Theoretical procedure p2 (see Calculation procedures section).
[b] $\Delta_rG^\circ_T$ and[a]$\Delta_rH^\circ_T$ values for the hydrogenation reaction
[c] Equilibrium constants for dehydrogenation reaction, $K_d = 1/K_h$ (see Scheme 1, $ER_h \rightarrow nH_2 + EL_d$). Equilibrium constants for hydrogenation reaction, $K_h = e^{\frac{-\Delta_rG^\circ_T}{RT}}$. (all of values of K_d and K_h are shown in SM-II).
[d] Theoretical dehydrogenation equilibrium yields (% ε_d) calculated from K_d values and the polynomial equations of the dehydrogenation equilibrium ($n^2\,\varepsilon_d^{n+1} + K_d\,\varepsilon_d - K_d = 0$, % $\varepsilon_d = 100 \times \varepsilon_d$).
[e] 2,3-**DHT** is the only hydrogenated product.

are included in SM-II). Therefore, in reactions exhibiting a moderate % ε_d at mild temperatures, thermodynamic reversibility could be facilitated for the applications as LOHCs.

The incorporation of a methyl group (Me) on any position of **Pyrr** and **T** increased $\Delta_rH^\circ_{453K}$ and $\Delta_rG^\circ_{453K}$ values for hydrogenation reaction (see reactions 40–42 in Tables 3 and [64,65] in Table 4). A similar behavior was observed for the substitution with other groups (see Tables 3 and 4). According to these results, substitution by any R group displaced the equilibrium towards dehydrogenation reactions. The alkyl substitution (Me, Et and Pr) on **Pyrr** allowed to improve the dehydrogenation process (K_d from ~10^{-2} to ~10^{-1}).

Particularly, the substitution of an alkyl group in the 1-position of **Pyrr** produced important differences in the K_d values (see reactions 5, 40–48); these changes managed to improve the hydrogen release process with moderate % ε_d values (from 33.8% to 43.9%). However, the change of Me by Pr decreased hydrogen storage capacity from 4.7 %wt H for the pair 1-**MePyrr**/1-**MeTHPyrr** (reaction 40) to 3.6 %wt H in the pair 1-Pr**Pyrr**/1-Pr**THPyrr** (reaction 46 in Table 3). Although the K_d values increase with alkyl substitution on **T** (see reactions 64–73 in Table 4), the magnitudes of the K_d (from ~10^{-9} to ~10^{-7}) showed to be low for practical applications of LOHCs.

The incorporation of unsaturated substituent groups containing isolated double (vinyl) or triple (ethynyl) on **Pyrr** gave K_d similar values compared to those obtained for alkyl substitution (see reactions 49–54 of Table 3). The substitution of an allyl group in 3-position on Pyrr produced an endergonic hydrogenation reaction which occurred for the first time ($\Delta_rG^\circ_{453K} = 5.1$ kJ mol^{-1}, reaction 57, Table 3). Consequently, at 453 K ($K_d = 3.8$) under the equilibrium conditions of reaction 57, the release of hydrogen was favored (% $\varepsilon_d = 67.8$%) and the

Please cite this article as: Izquierdo R et al., Substituted heterocycles as new candidates for liquid organic hydrogen carriers: *In silico* design from DFT calculations, International Journal of Hydrogen Energy, https://doi.org/10.1016/j.ijhydene.2021.02.201

Table 4 – Thermodynamic functions (kJ mol^{-1}) for the hydrogenation of thiophenes calculated from M06-HF/6–31(d) at 453 K and 1 bar.

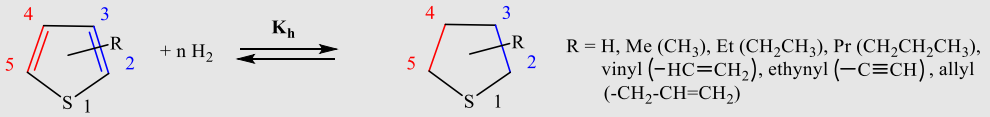

N	Reagent	bp (K)[a]	n	Product	bp (K)	$\Delta_rG^\circ_T(\Delta_rH^\circ_T)$[d]	K_d[c]	%wt H	% ε_d[d]
(6)	**T**	358[a1]	1	2,3-**DHT**[e]	404[a1]	−5.9 (−59.2)	2.1×10^{-1}	2.3	36.4
(7)	**T**	358[a1]	2	**THT**	394[a1]	−85.2 (−197.1)	1.5×10^{-10}	4.6	~0.0
(64)	2-Me**T**	387[a1]	2	2-Me**THT**	405[a1]	−73.3 (−193.1)	3.6×10^{-9}	3.9	0.1
(65)	3-Me**T**	390[a1]	2	3-Me**THT**	406[a2]	−76.1 (−194.8)	1.7×10^{-9}	3.9	0.1
(66)	2-Et**T**	407[a1]	2	2-Et**THT**	428[a2]	−75.2 (−192.7)	2.1×10^{-9}	3.5	0.1
(67)	3-Et**T**	413[a1]	2	3-Et**THT**	438[a2]	−70.7 (−187.9)	7.1×10^{-9}	3.5	0.1
(68)	2-Pr**T**	433[a1]	2	2-Pr**THT**	450[a2]	−60.3 (−180.6)	1.1×10^{-7}	3.1	0.3
(69)	3-Pr**T**	438[a1]	2	3-Pr**THT**	438[a3]	−56.4 (−176.4)	3.2×10^{-7}	3.1	0.4
(70)	2-vinyl**T**	400[a1]	2	2-vinyl**THT**	424[a2]	−72.7 (−188.7)	4.2×10^{-9}	3.5	0.1
(71)	3-vinyl**T**	425[a2]	2	3-vinyl**THT**	424[a2]	−66.6 (−184.7)	2.1×10^{-8}	3.5	0.2
(72)	2-ethynyl**T**	426[a1]	2	2-ethynyl**THT**	410[a3]	−72.0 (−187.1)	5.0×10^{-9}	3.6	0.1
(73)	3-ethynyl**T**	426[a1]	2	3-ethynyl**THT**	426[a2]	−74.9 (−189.8)	2.3×10^{-9}	3.6	0.1
(74)	2-allyl**T**	430[a1]	2	2-allyl**THT**	430[a3]	−79.4 (−197.3)	7.0×10^{-10}	3.1	0.1
(75)	3-allyl**T**	430[a2]	2	3-allyl**THT**	448[a1]	−74.6 (−190.9)	2.5×10^{-9}	3.1	0.1
(76)	2-vinyl**T**	400[a1]	3	2-Et**THT**	407[a2]	−155.3 (−330.8)	1.3×10^{-18}	5.2	~0.0
(77)	3-vinyl**T**	425[a1]		-Et**THT**	413[a1]	−148.8 (−324.2)	7.0×10^{-18}	5.2	~0.0
(78)	2-allyl**T**	430[a1]	3	2-Pr**THT**	433[a1]	−149.8 (−328.2)	5.4×10^{-18}	4.6	~0.0
(79)	3-allyl**T**	430[a1]	3	3-Pr**THT**	434[a1]	−144.3 (−321.2)	2.3×10^{-17}	4.6	~0.0

[b] $\Delta_rG^\circ_T$ and $\Delta_rH^\circ_T$ values for the hydrogenation reaction.
[a] Boiling point.
[a1] Experimental.
[a2] Theoretical procedure p1.
[a3] Theoretical procedure p2 (see Calculation procedures section).
[c] Equilibrium constants for dehydrogenation reaction, $K_d = 1/K_h$ (see Scheme 1, $ER_h \rightarrow nH_2 + EL_d$). Equilibrium constants for hydrogenation reaction, $K_h = e^{\frac{-\Delta_rG^\circ_T}{RT}}$. (all of values of K_d and K_h are shown in SM-II).
[d] Theoretical dehydrogenation equilibrium yields (% ε_d) calculated from K_d values and the polynomial equations of the dehydrogenation equilibrium ($n_2\,\varepsilon_d^{n+1} + K_d\,\varepsilon_d - K_d = 0$, % $\varepsilon_d = 100 \times \varepsilon_d$).
[e] 2,3-DHT is the only hydrogenated product.

3-allyl**Pyrr**/3-allyl**THPyrr** pair could have some application as LOHC. The hydrogen storage capacity of 3.6 %wt of the 3-allyl**Pyrr**/3-allyl**THPyrr** pair could guide its use as LOHC for both stationary energy storage and energy transport; however, the %wt H value was slightly low for mobile applications.

The presence of an additional unsaturated substituent, i.e. allyl group giving two more sites for hydrogen atoms, is an alternative to improve the hydrogen storage capacities in the EL_d state (**Pyrr**). Particularly, the increasing storage capacity by changing the 3-allyl**Pyrr**/3-allyl**THPyrr** pair ($K_d = 3.8$, 3.6 %wt H, reaction 57) to the 3-allyl-**P**/3-Pr-**THPyrr** pair ($K_d = 2.7 \times 10^{-11}$, 5.3 %wt H, reaction 63) did not improve the dehydrogenation thermodynamics, which is key process for LOHC applications, consequently the % ε_d value decrease to 0.1% (see reaction groups 55–57 and 61–63 for all the -allyl substitutions). This result is similar to the conclusions reported by Jessop et al. [33], who established at the DFT level (B3LYP/6-311G**) that the presence of a conjugated external substituent also had a lowering effect on the dehydrogenation enthalpy from 4-ethylpiperidine to 4-vinylpiperidine.

The thermodynamic condition for the reversibility is only obtained if the off-board substituent remains unsaturated after the hydrogenation. Apparently, one external unsaturated substituent would be easily hydrogenated to be a good choice; however, the presence of groups on the terminal carbon of the double bound could prevent hydrogenation of this unsaturation. Finally, the group of reactions 64–79 showed K_d and %wt H values which indicate that regardless the storage capacity and the substitutions of the pairs EL_d/ER_h related with **T**, these compounds are not useful for developing new LOHCs.

According to reactions 5 and 6, the **Pyrr/THPyrr** and **T/2,3-DHT** pairs showed favorable thermodynamics for reversible hydrogenation/dehydrogenation of four (**n** = 2, see Scheme 1) and two (**n** = 1) hydrogen atoms, respectively. At low temperatures (298 K), hydrogenation reaction was favored (see Table 2, reactions 5 and 6), while at high temperatures (453 K) there are improvements in the dehydrogenation reaction (see Table 3 reactions 5 and Table 4 reaction 6). Therefore, the temperature could be the thermodynamic switch for storing and releasing hydrogen. Despite their appropriate thermodynamic behavior, the **Pyrr/THPyrr** and **T/2,3-DHT** pairs presented moderate (5.7 %wt H) and low (2.3 %wt H) storage capacities, respectively (see Tables 3 and 4).

Please cite this article as: Izquierdo R et al., Substituted heterocycles as new candidates for liquid organic hydrogen carriers: *In silico* design from DFT calculations, International Journal of Hydrogen Energy, https://doi.org/10.1016/j.ijhydene.2021.02.201

Table 5 – Thermodynamic functions for the hydrogenation of thienyl-pyrroles calculated from M06-HF/6–31(d) at 453 K and 1 bar.

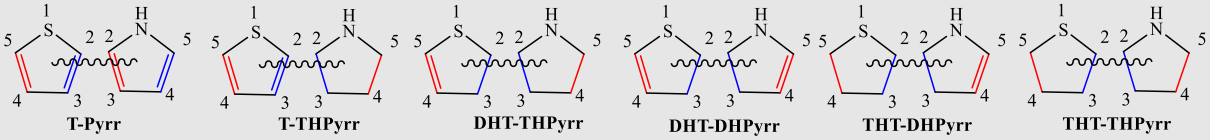

N[a]	Reagent (R_i)	bp(K)[b]	Product	bp(K)[b]	$\Delta_r G^\circ_T(\Delta_r H^\circ_T)$	K_d[c]	% ε_d[d]
(80)	1 (T-2)-Pyrr	517[b1]	1 (T-2)-THPyrr	519[b2]	−26.6 (−143.0)	8.6×10^{-4}	5.9
(81)	2 (T −2)-Pyrr	576[b1]	2 (T-2)-THPyrr	518[b1]	−14.6 (−127.0)	2.1×10^{-2}	16.3
(82)	3 (T −2)-Pyrr	554[b2]	3 (T-2)-THPyrr	494[b3]	−6.2 (−123.6)	1.9×10^{-1}	32.0
(83)	1 (DHT-2)-Pyrr	507[b2]	1 (2,3-DHT-2)-THPyrr	458[b3]	−11.6 (−132.2)	4.6×10^{-2}	20.9
(84)	2 (DHT-2)-Pyrr	524[b2]	2 (2,3-DHT-2)-THPyrr	472[b3]	−16.6 (−135.7)	1.2×10^{-2}	13.8
(85)	3 (DHT-2)-Pyrr	554[b2]	3 (2,3-DHT-2)-THPyrr	472[b3]	−3.5 (−123.9)	3.9×10^{-1}	39.2
(86)	1 (THT-2)-Pyrr	507[b2]	1 (THT-2)-THPyrr	468[b3]	−29.6 (−150.0)	3.9×10^{-4}	4.5
(87)	2 (THT-2)-Pyrr	528[b2]	2 (THT-2)-THPyrr	488[b3]	−25.4 (−144.8)	1.2×10^{-3}	6.5
(88)	3 (THT-2)-Pyrr	554[b2]	3 (THT-2)-THPyrr	526[b2]	−10.0 (−129.7)	7.0×10^{-2}	23.8
(89)	1 (T-2)-Pyrr	517[b1]	1 (2,3-DHT-2)-2,3-DHPyrr	445[b3]	28.5 (−87.0)	1.9×10^{3}	99.8
(90)	1 (T-2)-Pyrr	517[b1]	1 (4,5-DHT-2)-2,3-DHPyrr	469[b3]	11.9 (−96.0)	2.4×10^{1}	88.3
(91)	1 (T-3)-Pyrr	518[b1]	1 (DHT-3)-2,3-DHPyrr	436[b3]	35.6 (−79.5)	1.3×10^{4}	100.0
(92)	1 (T-3)-Pyrr	518[b1]	1 (4,5-DHT-3)-2,3-DHPyrr	469[b3]	21.9 (−88.7)	3.3×10^{2}	98.8
(93)	2 (T-2)-Pyrr	576[b1]	2 (2,3-DHT-2)-2,3-DHyrr	468[b3]	45.9 (−67.6)	2.0×10^{5}	100.0
(94)	2 (T 2)-Pyrr	576[b1]	2 (4,5-DHT-2)-4,5-DHPyrr	481[b3]	36.7 (−77.4)	1.7×10^{4}	100.0
(95)	2 (T 2)-Pyrr	576[b1]	2 (2,3-DHT-2)-4,5-DHPyrr	477[b3]	54.6 (−58.3)	2.0×10^{6}	100.0
(96)	2 (T-2)-Pyrr	576[b1]	2 (2,3-DHT-2)-2,3-DHPyrr	477[b3]	49.8 (−64.5)	5.5×10^{5}	100.0
(97)	2 (T-3)-Pyrr	543[b1]	2 (2,3-DHT-3)-2,3-DHPyrr	468[b3]	45.3 (−73.3)	1.7×10^{5}	100.0
(98)	2 (T-3)-Pyrr	543[b1]	2 (2,3-DHT-3)-2,3-DHPyrr	477[b3]	55.2 (−58.7)	2.3×10^{6}	100.0
(99)	2 (T-3)-Pyrr	543[b1]	2 (2,3-DHT-3)-4,5-DHPyrr	496[b3]	34.6 (−78.8)	9.7×10^{3}	100.0
(100)	2 (T-3)-Pyrr	543[b1]	2 (2,3-DHT-3)4,5-DHPyrr	477[b3]	43.4 (−70.0)	1.0×10^{5}	100.0
(101)	3 (T-2)-Pyrr	578[b1]	3 (2,3-DHT-2)-2,3-DHPyrr	473[b3]	54.4 (−63.3)	1.9×10^{6}	100.0
(102)	3 (T-2)-Pyrr	578[b1]	3 (2,3-DHT-2)-4,5-DHPyrr	486[b3]	33.3 (−80.2)	6.9×10^{3}	99.9
(103)	3 (T-2)-Pyrr	578[b1]	3 (2,3-DHT-2)-4,5-DHPyrr	492[b3]	52.0 (−61.8	9.9×10^{5}	100.0
(104)	1 (T-2)-Pyrr	517[b1]	1 (4,5-DHT-2)-THPyrr	469[b3]	−15.0 (−190.9)	1.9×10^{-2}	20.3
(105)	1 (T-2)-Pyrr	517[b1]	1 (THT-2)-2,3-DHPyrr	458[b3]	−51.0 (−221.9)	1.3×10^{-6}	1.9
(106)	2 (T-2)-Pyrr	576[b1]	2 (DHT-2)-THPyrr	524[b3]	−9.6 (−182.2)	7.8×10^{-2}	28.1
(107)	2 (T-2)-Pyrr	576[b1]	2 (THT-2)-2,3-DHPyrr	496[b3]	29.6 (−201.3)	3.9×10^{-4}	8.2
(108)	3 (T-2)-Pyrr	578[1b1]	3 (4,5-DHT-2)-THPyrr	476[b3]	−16.6 (−184.0)	1.2×10^{-2}	18.2
(109)	3 (T-2)-Pyrr	578[1b1]	3 (THT-2)-2,3-DHP	472[b3]	−24.7 (−202.1)	1.4×10^{-3}	10.9
(110)	1 (T-2)-Pyrr	517[b1]	1 (THT-2)-THPyrr	468[b3]	−94.1 (−328.3)	1.4×10^{-11}	0.4
(111)	2 (T-2)-Pyrr	576[b1]	2 (THT-2)-THPyrr	525[b2]	−93.8 (−327.6)	1.5×10^{-11}	0.4
(112)	3 (T-2[d]Pyrr	578[b1]	3 (THT-2)-THPyrr	526[b2]	−79.6 (−314.4)	6.7×10^{-10}	0.8

[a] Reactions 80–103: n = 2, %wt H = 2.6; Reactions 104–109: n = 3, %wt H = 3.9; Reactions 110–112: n = 4, %wt H = 5.1.
[b] Boiling point.
[b1] Experimental.
[b2] Theoretical procedure p1 and.
[b3] Theoretical procedure p2 (see Calculation procedures section).
[c] Equilibrium constants for dehydrogenation reaction, $K_d = 1/K_h$ (see Scheme 1, $ER_h \rightarrow nH_2 + EL_d$). Equilibrium constants for hydrogenation reaction, $K_h = e^{\frac{-\Delta_r G^\circ_T}{RT}}$ (all of values of K_d and K_h are shown in SM-II).
[d] Theoretical dehydrogenation equilibrium yields (% ε_d) calculated from K_d values and the polynomial equations of the dehydrogenation equilibrium ($n^2\,\varepsilon_d^{n+1} + K_d\,\varepsilon_d - K_d = 0$, % $\varepsilon_d = 100 \times \varepsilon_d$).

An improvement of the thermodynamic properties and the hydrogen storage capacities can be reached by combining the pairs **Pyrr/THPyrr** and **T**/2,3-**DHT** by chemical linking of both the EL_d (**Pyrr** and **T**) and ER_h (**THPyrr** and **T** or 2,3-**DHT**). For example, the chemical linking of one 2-thienyl group (**T-2**) in the 2-position in pyrrole (**Pyrr**) produces the molecule 2-(2-thiophen-2-yl)pyrrole labeled here "2 (**T**-2)-**Pyrr**", which could be a new LOHC. Scheme 4 shows six (6) thienyl-pyrroles that could be used as possible LOHCs. Also, the structures and names of all the thienyl-pyrroles used in this work are listed in the Supplementary Material III (SM-III). Simple synthetic procedures for generating a covalent bond between positions 1, 2 and 3 in pyrroles and 2 and 3 in thiophenes are well known. Trofimov et al. [71] and Joule [72] reviewed the synthesis methods for bi-pyrroles, furyl- and thienyl-pyrroles. In these works, some of those compounds were selected to be studied from the thermodynamic viewpoint and their applications as possible LOHCs.

Please cite this article as: Izquierdo R et al., Substituted heterocycles as new candidates for liquid organic hydrogen carriers: *In silico* design from DFT calculations, International Journal of Hydrogen Energy, https://doi.org/10.1016/j.ijhydene.2021.02.201

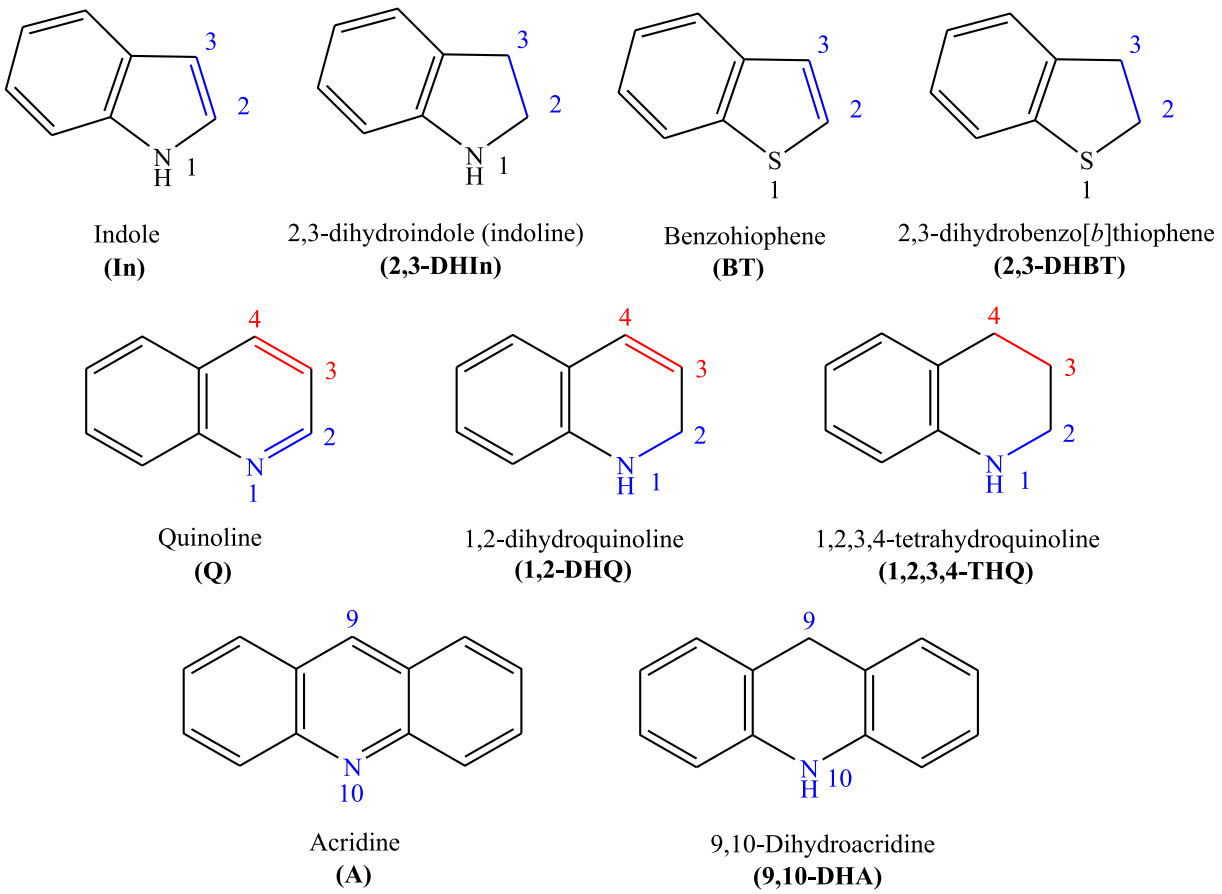

Scheme 3 – Proposed fused heterocycle compounds.

Table 5 shows the most featured thermodynamic data for hydrogenation reactions of the thienyl-pyrrole systems. The substitution of the fragments thienyl (**T-**), 2,3-dihydrothienyl (**DHT-**) and tetrahydrothienyl (**THT-**) on positions 1 and 2 in pyrrole (**Pyrr**) showed K_d values at 453 K that are not suitable for storage hydrogen applications (see reactions 80–88). Under these conditions, the enthalpy control ($|\Delta_r H^\circ_T| > |T\Delta_r S^\circ_T|$) dominated these reactions and it would not be so easy to release **2** H_2 molecules (Scheme 1 and Table 5) from these materials. The substitution in positions 3 produces the EL_d/ER_h pairs 3 (**T** –2)-**Pyrr**/3 (**T**-2)-**THPyrr**, 3 (**T**-2)-**Pyrr**, 3 (**DHT**-2)-**Pyrr**/3 (**DHT**-2)-**THPyrr** and 3 (**THT**-2)-**Pyrr**/3 (**THT**-2)-**THPyrr**, which had moderate efficiencies for the dehydrogenation process of (% ε_d from 23.8 to 39.2). This behavior was observed in the allyl substitutions in pyrrole, apparently the substitutions of groups on the 3 position of the pyrrole favor hydrogen release.

On the other hand, the partial hydrogenation in both the pyrrolyl and thienyl fragments gave favorable K_d values ($K_d >> 10$) for LOHC applications (see reactions 89–103). The % ε_d-values for these reactions were greater than 88%, which seem to indicate that these ER_h based on the linked between **DHPyrr** and **DHT** could be used successfully to release **2**-H_2 molecules (i.e. see 2 (**DHT**-2)-**DHPyrr** structure in Scheme 4 and SM-III). Despite the low hydrogen storage for reactions 89–103 (low % wt H, limiting their applications in vehicular LOHCs), the high K_d values suggested an interesting potential use in stationary hydrogen storage applications (off-board). In these applications, the size of the EL_d/ER_h container is less important than the thermodynamic efficiency.

The reactions 104–109 showed moderate K_d values obtained by including total and partial hydrogenation in the fragments pyrrolyl and thienyl. Additionally, the inclusion of total hydrogenation reactions in both fragments reduced the K_d values (see reactions 110–112). In this group of candidates, only the 2 (**T**-2)-**Pyrr**/2 (**DHT**-2)-**DHP** pair (Scheme 4) presents a moderate efficiency to release hydrogen according to the reaction in equilibrium 106 (% $\varepsilon_d = 28.1\%$ and **n** = 3 in Scheme 1).

Fig. 2 shows the % ε_d at 1 bar in the range from 298 K to 453 K for the dehydrogenation of some EL_d/ER_h pairs as LOHC candidates. The **Pyrr**/**THP** and **T**/**THT** pairs released hydrogen with low efficiency (% $\varepsilon_d < 1\%$), the equilibrium concentration measured as mole fraction of hydrogen released ($\chi_{(H2)}$) was less than 0.1. At the optimal temperature range for mobile applications these pairs exclusively work in the hydrogen storage zone (see Fig. 2), and only the hydrogenation reaction is favored (see reactions 5 and 6 to the right).

In the range from 298 K to 453 K the 2 (**T**-2)-**Pyrr**/2 (**DHT**-2)-**DHPyrr** pair could be useful for hydrogen release only (% $\varepsilon_d > 80\%$). Therefore, this pair is in the hydrogen release zone (see Fig. 2, % $\varepsilon_d = 100\%$ at 453 K) and the reaction 93 is highly

Please cite this article as: Izquierdo R et al., Substituted heterocycles as new candidates for liquid organic hydrogen carriers: *In silico* design from DFT calculations, International Journal of Hydrogen Energy, https://doi.org/10.1016/j.ijhydene.2021.02.201

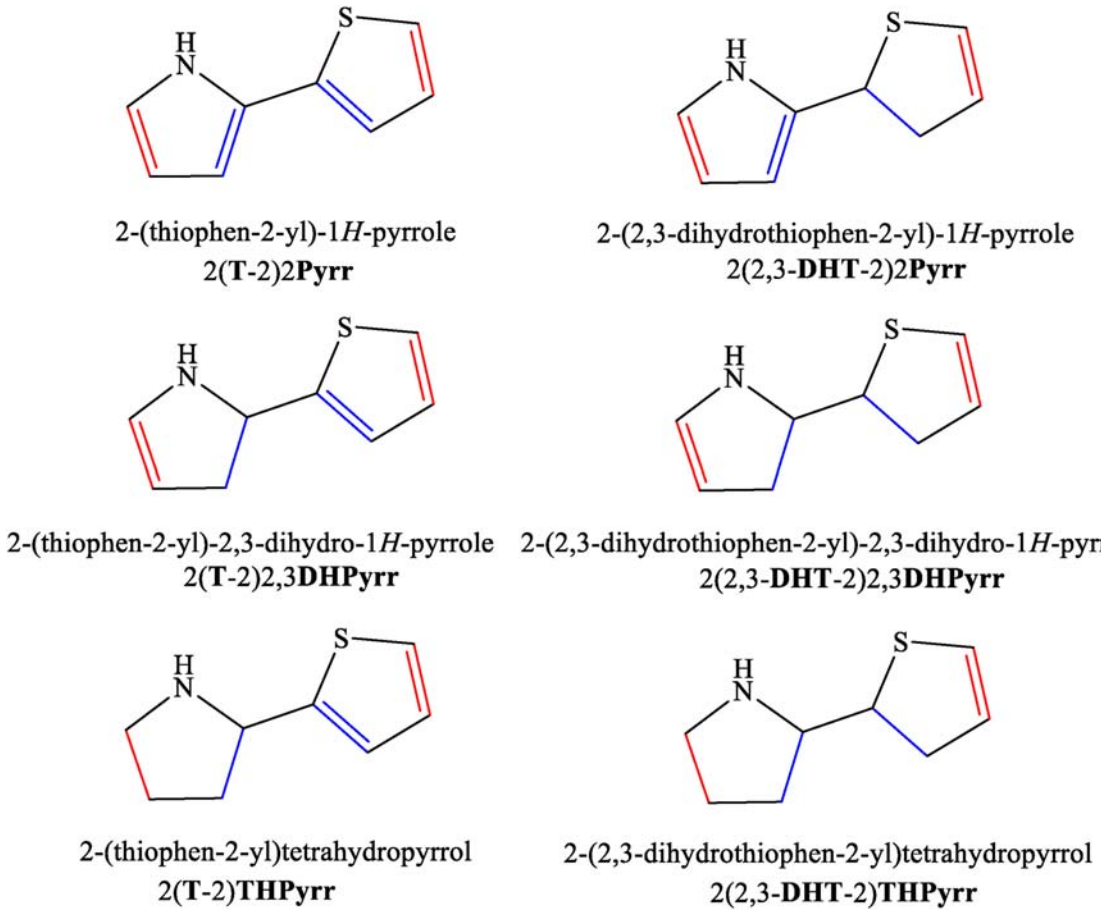

Scheme 4 – Some hybrid materials based on thienyl-pyrroles as candidates for LOHCs.

favored to the left. The trend for the 2(T-2)-**Pyrr**/2(DHT-2)-**DHPyrr** pair in Fig. 2 indicate that low temperatures (<< 298 K) are necessary to make hydrogen loading in the ER_h state feasible.

On the other hand, at 453 K, the 3-allyl-**Pyrr**/3-allyl-**THPyrr** and 2 (T-2)-**Pyrr**/2 (DHT-2)-**THPyrr** pairs presented the moderate efficiencies with % ε_d values from 28.1% to 67.8% suitable for the "reversible hydrogen release". These efficiencies were like those obtained for the **T/DHT** pair (% $\varepsilon_d = 36.4$) but with higher theoretical hydrogen storage (see %wt H in reaction 6, 57 and 106). The 3-allyl-**Pyrr**/3-allyl-**THPyrr** and 2 (T-2)-**Pyrr**/2 (DHT-2)-**THPyrr** pairs presented K_d values from 0.078 to 3.9 very close to the ideal reversibility (K_d ~ 1) which is fundamental for the good performance of catalysts in LOHCs [18,45,73].

Safronov et al. [53] recently reported similar theoretical results for pyrazole derivatives as potentials LOHC. Based on their results with chemical accuracy at the G4 level, they proposed the 1-phenylpyrazole/1-cyclohexylpyrazolidine pair as the best candidate for LOHC. At DFT level (M06HF/6-31G*), it was possible to obtain an enthalpy value ($\Delta_r H^{\circ}_{298K}$) for hydrogenation from 1-phenylpyrazole to 1-cyclohexylpyrazolidine of −252.0 kJ mol^{-1} with an error (%E_r) of 5.3% compared to G4 reference [53]. At 453 K, we obtained a K_d value of 1.8×10^3 for the 1 phenylpyrazole to 1-cyclohexylpyrazolidine pair. In contrast to the 3-allyl-**Pyrr**/3-allyl-**THPyrr** and 2 (T-2)**Pyrr**/2 (2,3-**DHT**-2)**THPyrr** pairs, the 1-phenylpyrazole/1-cyclohexyl pyrazolidine pair would only be positioned in the hydrogen release zone and this pair could hardly be obtained naturally or from oil-refining by-products.

Finally, the change in temperatures from 298 K to 453 K achieved reversible hydrogenation/dehydrogenation between the 3-allyl-**Pyrr**/3-allyl-**THPyrr** and 2 (**T**-2)**Pyrr**/2 (2,3-**DHT**-2) **THPyrr** pairs (LOHC zone, see yellow color in Fig. 2). Subtle changes in temperature managed to switch the EL_d states to ER_h and *vice versa*. This is a very desirable feature in LOHCs.

Alkyl or alkenyl substitutions on the **Pyrr**/**THPyrr** and **T**/**THT** pairs produced significant changes in the bp of candidate LOHCs. In particular, allyl substitution in position 3 on **Pyrr**/**THPyrr** pair to produce 3-allyl-**Pyrr**/3-allyl-**THPyrr** pair increases the bp in the EL_d and ER_h of the new LOHC from 402 K (**Pyrr**) and 393 K (**THPyrr**) to 453 K (3-allyl-**Pyrr**) and 425 K (3-allyl-TH**Pyrr**). Despite optimal efficiency for hydrogen discharge at 453 K (% $\varepsilon_d = 67.8\%$, see Fig. 2), the bp of 3-allyl-**Pyrr**/3-allyl-**THPyrr** pair were still low and evaporation would be significant to be used on-board vehicle. Thus, to improve the manageability of 3-allyl-Pyrr/3-allylTHPyrr pair, it is required to lower the temperature in the dehydrogenation process to 420 K maintaining moderate % ε_d values (~40%, see Fig. 2). An aspect that should be highlighted in this point is that although under hydrogenation conditions both the carbon-carbon double bonds of **Pyrr**

Please cite this article as: Izquierdo R et al., Substituted heterocycles as new candidates for liquid organic hydrogen carriers: *In silico* design from DFT calculations, International Journal of Hydrogen Energy, https://doi.org/10.1016/j.ijhydene.2021.02.201

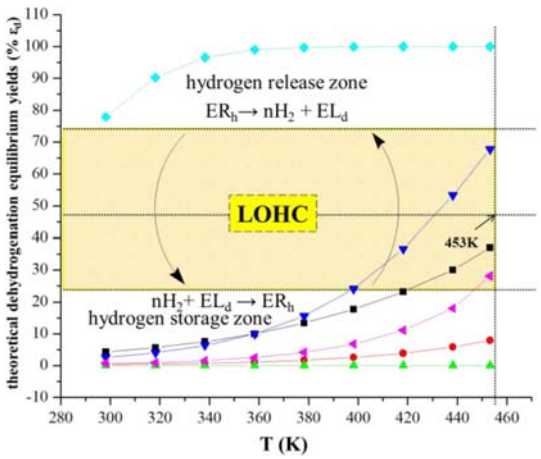

Fig. 2 – Theoretical dehydrogenation equilibrium conditions: $ER_h \rightarrow nH_2 + EL_d$. Pairs: (■) T/2,3-DHT; (●) P/2,3-DHP; (▲) T/THT; (▼) 3-allyl-P/3-allyl-THP; (◀) 2(T-2)-P/2(2,3-T-2)-THP; (♦) 2(T-2)-P/2(2,3-DHT-2)2,3-DHP.

and the one of the allyl group should be hydrogenated, it is possible to avoid the hydrogenation of the C=C bond of the allyl group introducing substituents in the terminal carbon of the allyl group.

The **2(T-2)Pyrr/2(2,3-DHT-2)THPyrr** pair presented bp above 70 K in relation to the dehydrogenation temperatures (453 K), so both EL_d and ER_h are liquid state at all stages of hydrogenation (storage)/dehydrogenation (release) of hydrogen, this avoid the separation processes and some transport issues.

Finally, molecular electronics gives insights into the molecular origin of a chemical process. Remarkably, the charge transfer between HOMO and LUMO orbitals can describe the reactivity of a compound towards a specific reaction. In this sense, we have carried out a preliminary analysis based on Frontier Molecular Orbitals (FMO) of the reversible hydrogenation/dehydrogenation reactions of the 3-allyl**Pyrr**/3-allyl**THPyrr** and 2 (**T**-2)-**Pyrr**/2 (2,3-**DHT**-2)-**THPyrr** pairs, which are promising candidates for chemical hydrogen storage. Particularly, the charge transfer between HOMO and LUMO orbitals is capable to describe the reactivity of a compound towards a specific reaction. Fig. 3a shows the HOMO, LUMO and energy gaps for these two promising EL_d/ER_h pairs; two non-promising pairs (cyclopentadiene/cyclopentane and **Pyrr**/**THPyrr**) are including for comparison (Fig. 3b). All of the non-hydrogenated molecules contain the HOMO delocalized on the double bond skeleton bearing a conjugated π system. On the other hand, the LUMO for cyclopentadiene, **Pyrr** and **2(T-2)Pyrr** are located on the atoms participating in the double bonds as antibonding π orbitals. According to FMO theory, the charge transfer from HOMO to LUMO can be related to the double-bond breaking and, consequently, the hydrogenation process [74]. In 3-allylPyrr, the LUMO is spatially located on allyl double bond. This result seems to indicate that there is a significant reactivity point on the allyl group. Therefore, it is important in the future to consider the protection of the allyl group for the use of the 3-allyl**Pyrr**/3-allyl**THPyrr** pair as LOHCs.

In the hydrogenated molecules for the non-promising pairs, cyclopentane and **THPyrr**, the HOMO and LUMO are spatially distributed to the diverse C–C, C–H and C–N bonds, as σ and σ^* orbitals. In the case of hydrogenated molecules of the promising pairs, only the HOMO for 3-allyl**THPyrr** has a similar behavior of the non-efficient pairs; while the HOMO for 2 (2,3-**DHT**-2)-**THPyrr** delocalizes on the π system of thiophene moiety.

On the order hand, the LUMO for each hydrogenated molecule of the promising pairs are differents. For 3-allyl**THPyrr**, they are distributed on the allyl double bond, while 2 (2,3-**DHT**-2)-**THPyrr** delocalized on the thiophene fragment. In both cases, the shape of the orbitals indicates the antibonding nature of these orbitals. This behavior advises a potential reactivity. The HOMO-LUMO energy gaps for the ER_h (hydrogenate materials) of the four EL_d/ER_h pairs followed the

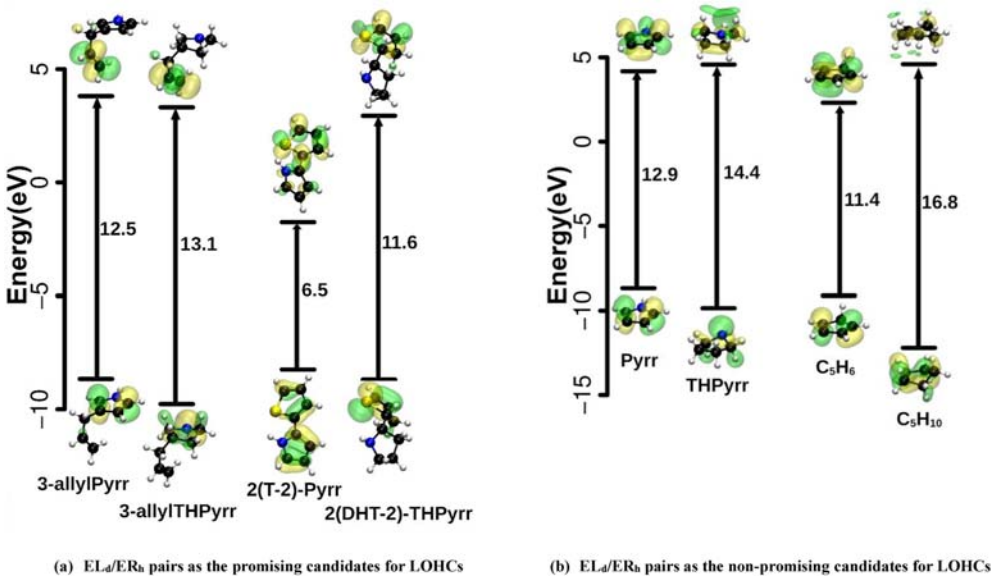

(a) EL_d/ER_h pairs as the promising candidates for LOHCs (b) EL_d/ER_h pairs as the non-promising candidates for LOHCs

Fig. 3 – Analysis of Frontier Molecular Orbitals (FMO) for some EL_d/ER_h pairs.

Please cite this article as: Izquierdo R et al., Substituted heterocycles as new candidates for liquid organic hydrogen carriers: *In silico* design from DFT calculations, International Journal of Hydrogen Energy, https://doi.org/10.1016/j.ijhydene.2021.02.201

trend: cyclopentane > **THPyrr** > 3-allyl**THPyrr** > 2 (2,3-**DHT**-2)-**THPyrr**. Assuming dehydrogenation also occurs by a HOMO-LUMO transfer, 3-allyl**THPyrr** and 2 (2,3-**DHT**-2)-**THPyrr** would be expected to release hydrogen (dehydrogenation reactions) more easily than cyclopentane and **THPyrr.** This result is in agreement with the K_d values. The 3-allyl**Pyrr**/3-allyl**THPyrr** and 2 (**T**-2)-**Pyrr**/2 (**DHT**-2)-**THPyrr** pairs present K_d values higher than the cyclopentadiene/cyclopentane and **Pyrr**/**THPyrr** pairs (see reactions sm3 in SM-I, 5, 57 and 106 in Tables 3 and 5, respectively). Although these results do not allow solving the catalytic challenge in these candidates for LOHCs, the approach of the FMO theory could contribute to improve understanding of the dehydrogenation reactions included in LOHC technologies. A similar approach was recently published by Govindaraja et al. [75], who used a deeper approach to FMO theory in the theoretical study of potential liquid organic hydrogen carriers based on dehydrogenation of ethylene diamine monoborane adducts and their cyclic products.

Conclusions

By using DFT theoretical calculations, the thermodynamic and physicochemical properties of some pairs EL_d/ER_h based on heterocyclic compounds were examined, which showed to have possible application in HST. Among the most important conclusions we can highlight the following four aspects:

(i) For reactions that include pyrrole and thiophene, the HF exchange level in global hybrid functionals is essential for thermodynamic reaction functions calculation. Only M06-HF functional (X = 100) can reproduce the reference $\Delta_r H^\circ_{298K}$ value with % E_r < 5% (G3 (MP2).

(ii) For the reversible hydrogenation/dehydrogenation of the EL_d/ER_h pairs, generally the fused or non-fused five-membered heterocycle rings presented more viable $\Delta_r H^\circ_T$ and $\Delta_r G^\circ_T$ values than the six-membered heterocyclic rings.

(iii) The results found in the present work demonstrate the potential of the pairs **Pyrr**/**THPyrr** and **T**/**THT** as a structural basis to synthesize new and better LOHCs. Particularly, we recommend allyl substitution in 3-position on **Pyrr** (pyrrole) to produce the pair 3-allyl-**Pyrr**/3-allyl-**THPyrr.** Furthermore, we propose that the thienyl-pyrroles and their hydrogenation products could enhance the favorable physical, storage and toxicological properties in the new LOHCs. In particular, the 2 (**T**-2)**Pyrr**/2 (2,3-**DHT**-2)**THPyrr** pair is promising for the HSTs. Especially, the 2 (**T**-2)**Pyrr**/2 (2,3-**DHT**-2) **THPyrr** pair could perform well as LOHCs for stationary hydrogen storage applications (off-board) such as the stand-alone energy systems, back-up systems and solar or wind energy accumulators.

(iv) In perspective, the chemistry of pyrroles linked to five-membered aromatic heterocycles similar to thiophene is still in its infancy. Nonetheless, the currently available data on their properties allowed us to consider them and their derivatives as promising compounds for medicine, agriculture and industrial applications. In the industrial field, precise thermodynamic data are demanded for both hydrotreatment and new hydrogen storage systems. The obtained results provide important and precise theoretical thermodynamic measurements applicable in these fields.

As a final remark, we believe that the reversible hydrogenation/dehydrogenation of the pairs involving pyrrole and/or thiophene fragments may be efficiently performed by using homogeneous, biphasic liquid-liquid or, preferably, heterogeneous catalysts, under mild reaction conditions. However, the size and complexity of these catalytic systems is restrictive for G3 (MP2) or G4 calculations, therefore the DFT (M06-HF) combined with medium-sized base sets is presented as an excellent option to approach the theoretical study of LOHCs in the presence of catalysts. Each one of our research groups are working on all these aspects.

Declaration of competing interest

The authors declare that they have no known competing financial interests or personal relationships that could have appeared to influence the work reported in this paper.

Acknowledgments

The authors gratefully acknowledge Ernesto San Blas, Alexander Moronta and Alfonso Ballestas for reviewing and commenting on this paper. Likewise, we thank Gustavo Chacón for his great help in the graphics of this paper.

Appendix A. Supplementary data

Supplementary data to this article can be found online at https://doi.org/10.1016/j.ijhydene.2021.02.201.

REFERENCES

[1] Andersson J, Grönkvist S. Large-scale storage of hydrogen. Int J Hydrogen Energy 2019;44:11901–19. https://doi.org/10.1016/j.ijhydene.2019.03.063.

[2] Makepeace JW, He T, Weidenthaler C, Jensen TR, Chang F, Vegge T, et al. Reversible ammonia-based and liquid organic hydrogen carriers for high-density hydrogen storage: recent progress. Int J Hydrogen Energy 2019;44:7746–67. https://doi.org/10.1016/j.ijhydene.2019.01.144.

[3] Lankof L, Tarkowski R. Assessment of the potential for underground hydrogen storage in bedded salt formation. Int J Hydrogen Energy 2020;45:19479. https://doi.org/10.1016/j.ijhydene.2020.05.024. –92.

[4] González I, De Santiago F, Arellano LG, Miranda Á, Trejo A, Salazar F, et al. Theoretical modelling of porous silicon decorated with metal atoms for hydrogen storage. Int J Hydrogen Energy 2020;45:26321–33. https://doi.org/10.1016/j.ijhydene.2020.05.097.

[5] Schmidt O, Gambhir A, Staffell I, Hawkes A, Nelson J, Few S. Future cost and performance of water electrolysis: an expert

elicitation study. Int J Hydrogen Energy 2017;42:30470–92. https://doi.org/10.1016/j.ijhydene.2017.10.045.
[6] Ishaq H, Siddiqui O, Chehade G, Dincer I. A solar and wind driven energy system for hydrogen and urea production with CO2 capturing. Int J Hydrogen Energy 2021;46:4749–60. https://doi.org/10.1016/j.ijhydene.2020.01.208.
[7] Zhang Y, Fu J, Xie M, Liu J. Improvement of H2/O2 chemical kinetic mechanism for high pressure combustion. Int J Hydrogen Energy 2020;46:5799–811. https://doi.org/10.1016/j.ijhydene.2020.11.083.
[8] Abe JO, Popoola API, Ajenifuja E, Popoola OM. Hydrogen energy, economy and storage: review and recommendation. Int J Hydrogen Energy 2019;44:15072–86. https://doi.org/10.1016/j.ijhydene.2019.04.068.
[9] Harrison D, Welchman E, Chabal YJ, Thonhauser T. Materials for hydrogen storage. Handb. Clean energy syst.. Chichester, UK: John Wiley & Sons, Ltd; 2015. p. 1–19. https://doi.org/10.1002/9781118991978.hces222.
[10] Züttel A, Hirscher M, Panella B, Yvon K, Orimo S, Bogdanović B, et al. Hydrogen storage. Hydrog. As a futur. Energy carr.. Wiley; 2008. p. 165–263. https://doi.org/10.1002/9783527622894.ch6.
[11] Hirscher M, Yartys VA, Baricco M, Bellosta von Colbe J, Blanchard D, Bowman RC, et al. Materials for hydrogen-based energy storage – past, recent progress and future outlook. J Alloys Compd 2020;827:153548. https://doi.org/10.1016/j.jallcom.2019.153548.
[12] Züttel A. Hydrogen storage methods. Naturwissenschaften 2004;91:157–72. https://doi.org/10.1007/s00114-004-0516-x.
[13] Mananghaya MR, Santos GN, Yu D. Hydrogen adsorption of Ti-decorated boron nitride nanotube: a density functional based tight binding molecular dynamics study. Adsorption 2018;24:683–90. https://doi.org/10.1007/s10450-018-9971-0.
[14] Mananghaya MR. A simulation of hydrogen adsorption/desorption in metal-functionalized BN nanotube. Mater Chem Phys 2019;240:122159. https://doi.org/10.1016/j.matchemphys.2019.122159.
[15] Dawood F, Anda M, Shafiullah GM. Hydrogen production for energy: an overview. Int J Hydrogen Energy 2020;45:3847–69. https://doi.org/10.1016/j.ijhydene.2019.12.059.
[16] Eberle U, Felderhoff M, Schüth F. Chemical and physical solutions for hydrogen storage. Angew Chem Int Ed 2009;48:6608–30. https://doi.org/10.1002/anie.200806293.
[17] Markiewicz M, Zhang YQ, Bösmann A, Brückner N, Thöming J, Wasserscheid P, et al. Environmental and health impact assessment of Liquid Organic Hydrogen Carrier (LOHC) systems-challenges and preliminary results. Energy Environ Sci 2015;8:1035–45. https://doi.org/10.1039/c4ee03528c.
[18] Shimbayashi T, Fujita K ichi. Metal-catalyzed hydrogenation and dehydrogenation reactions for efficient hydrogen storage. Tetrahedron 2020;1–8. https://doi.org/10.1016/j.tet.2020.130946.
[19] Vivancos Á, Beller M, Albrecht M. NHC-based iridium catalysts for hydrogenation and dehydrogenation of N-heteroarenes in water under mild conditions. ACS Catal 2018;8:17–21. https://doi.org/10.1021/acscatal.7b03547.
[20] Clot E, Eisenstein O, Crabtree RH. Computational structure-activity relationships in H2 storage: how placement of N atoms affects release temperatures in organic liquid storage materials. Chem Commun 2007:2231. https://doi.org/10.1039/b705037b. –3.
[21] Teichmann D, Arlt W, Wasserscheid P, Freymann R. A future energy supply based on Liquid Organic Hydrogen Carriers (LOHC). Energy Environ Sci 2011;4:2767–73. https://doi.org/10.1039/c1ee01454d.
[22] Aakko-Saksa PT, Cook C, Kiviaho J, Repo T. Liquid organic hydrogen carriers for transportation and storing of renewable energy – review and discussion. J Power Sources 2018;396:803–23. https://doi.org/10.1016/j.jpowsour.2018.04.011.
[23] Li L, Manier H, Manier MA. Integrated optimization model for hydrogen supply chain network design and hydrogen fueling station planning. Comput Chem Eng 2020;134. https://doi.org/10.1016/j.compchemeng.2019.106683.
[24] Ajanovic A, Haas R. Prospects and impediments for hydrogen and fuel cell vehicles in the transport sector. Int J Hydrogen Energy 2021;46:10049–58. https://doi.org/10.1016/j.ijhydene.2020.03.122.
[25] Müller K, Völkl J, Arlt W. Thermodynamic evaluation of potential organic hydrogen carriers. Energy Technol 2013;1:20–4. https://doi.org/10.1002/ente.201200045.
[26] Metzger JO, Eissen M. Concepts on the contribution of chemistry to a sustainable development. Renewable raw materials. Compt Rendus Chem 2004;7:569–81. https://doi.org/10.1016/j.crci.2003.12.003.
[27] Shin BS, Yoon CW, Kwak SK, Kang JW. Thermodynamic assessment of carbazole-based organic polycyclic compounds for hydrogen storage applications via a computational approach. Int J Hydrogen Energy 2018;43:12158–67. https://doi.org/10.1016/j.ijhydene.2018.04.182.
[28] Zou YQ, von Wolff N, Anaby A, Xie Y, Milstein D. Ethylene glycol as an efficient and reversible liquid-organic hydrogen carrier. Nat Catal 2019;2:415–22. https://doi.org/10.1038/s41929-019-0265-z.
[29] He T, Pei Q, Chen P. Liquid organic hydrogen carriers. J Energy Chem 2015;24:587–94. https://doi.org/10.1016/j.jechem.2015.08.007.
[30] Dong Y, Yang M, Li L, Zhu T, Chen X, Cheng H. Study on reversible hydrogen uptake and release of 1,2-dimethylindole as a new liquid organic hydrogen carrier. Int J Hydrogen Energy 2019;44:4919–29. https://doi.org/10.1016/j.ijhydene.2019.01.015.
[31] Zhao HY, Oyama ST, Naeemi ED. Hydrogen storage using heterocyclic compounds: the hydrogenation of 2-methylthiophene. Catal Today 2010;149:172–84. https://doi.org/10.1016/j.cattod.2009.02.039.
[32] Hydrogen storage | Department of Energy, U.S. accessed, https://www.energy.gov/eere/fuelcells/hydrogen-storage. [Accessed 14 September 2020].
[33] Cui Y, Kwok S, Bucholtz A, Davis B, Whitney RA, Jessop PG. The effect of substitution on the utility of piperidines and octahydroindoles for reversible hydrogen storage. New J Chem 2008;32:1027–37. https://doi.org/10.1039/b718209k.
[34] Wei Z, Shao F, Wang J. Recent advances in heterogeneous catalytic hydrogenation and dehydrogenation of N-heterocycles. Chin J Catal 2019;40:980–1002. https://doi.org/10.1016/S1872-2067(19)63336-X.
[35] Releases | the world's first global hydrogen supply chain demonstration project - MITSUI & CO., LTD. accessed, https://www.mitsui.com/jp/en/release/2017/1224164_10832.html. [Accessed 17 September 2020].
[36] Hydrogenious technologies products & projects LOHC technology applications, Germany.
[37] Niermann M, Beckendorff A, Kaltschmitt M, Bonhoff K. Liquid organic hydrogen carrier (LOHC) – assessment based on chemical and economic properties. Int J Hydrogen Energy

Please cite this article as: Izquierdo R et al., Substituted heterocycles as new candidates for liquid organic hydrogen carriers: *In silico* design from DFT calculations, International Journal of Hydrogen Energy, https://doi.org/10.1016/j.ijhydene.2021.02.201

2019;44:6631–54. https://doi.org/10.1016/j.ijhydene.2019.01.199.
[38] Gregis G, Schaefer S, Sanchez JB, Fierro V, Berger F, Bezverkhyy I, et al. Characterization of materials toward toluene traces detection for air quality monitoring and lung cancer diagnosis. Mater Chem Phys 2017;192:374–82. https://doi.org/10.1016/j.matchemphys.2017.02.015.
[39] Onoda M, Nagano Y, Fujita K ichi. Iridium-catalyzed dehydrogenative lactonization of 1,4-butanediol and reversal hydrogenation: new hydrogen storage system using cheap organic resources. Int J Hydrogen Energy 2019;44:28514–20. https://doi.org/10.1016/j.ijhydene.2019.03.219.
[40] Verevkin SP, Siewert R, Pimerzin AA. Furfuryl alcohol as a potential liquid organic hydrogen carrier (LOHC): thermochemical and computational study. Fuel 2020;266:117067. https://doi.org/10.1016/j.fuel.2020.117067.
[41] Tang C, Fei S, Lin GD, Liu Y. Natural liquid organic hydrogen carrier with low dehydrogenation energy: a first principles study. Int J Hydrogen Energy 2020;45:32089–97. https://doi.org/10.1016/j.ijhydene.2020.08.143.
[42] Fan-Chiang TT, Wang HK, Hsieh JC. Synthesis of phenanthridine skeletal Amaryllidaceae alkaloids. Tetrahedron 2016;72:5640–5. https://doi.org/10.1016/j.tet.2016.07.065.
[43] Pez GP, Scott AR, Raymond A, Cooper AC, Cheng H. USA Pat.; 2005. 0106, 2005.
[44] Crabtree RH. Hydrogen storage in liquid organic heterocycles. Energy Environ Sci 2008;1:134–8. https://doi.org/10.1039/b805644g.
[45] Li H, Jiang J, Lu G, Huang F, Wang Z. Onthe "reverse Gear"Mechanismof the reversible dehydrogenation/hydrogenation of a nitrogen heterocycle catalyzed by a cp*Ir complex: a computational study. Organometallics 2011;30:3131–41. https://doi.org/10.1021/om200222j.
[46] Moores A, Poyatos M, Luo Y, Crabtree RH. Catalysed low temperature H2 release from nitrogen heterocycles. New J Chem 2006;30:1675–8. https://doi.org/10.1039/b608914c.
[47] Vitaku E, Smith DT, Njardarson JT. Analysis of the structural diversity, substitution patterns, and frequency of nitrogen heterocycles among U.S. FDA approved pharmaceuticals. J Med Chem 2014;57:10257–74. https://doi.org/10.1021/jm501100b.
[48] Pathania S, Narang RK, Rawal RK. Role of sulphur-heterocycles in medicinal chemistry: an update. Eur J Med Chem 2019;180:486–508. https://doi.org/10.1016/j.ejmech.2019.07.043.
[49] Bianchini C, Meli A, Vizza F. Modelling the hydrodenitrogenation of aromatic N-heterocycles in the homogeneous phase. Eur J Inorg Chem 2001;2001:43–68. https://doi.org/10.1002/1099-0682(20011)2001:1<43::AID-EJIC43>3.0.CO. 2-9.
[50] Reynolds MA, Guzei IA, Logsdon BC, Thomas LM, Jacobson RA, Angelici RJ. Transition metal complexes of chromium, molybdenum, tungsten, and manganese containing η 1(S)-2,5-dimethylthiophene, benzothiophene, and dibenzothiophene ligands. Organometallics 1999;18:4075–81. https://doi.org/10.1021/om990322f.
[51] Zepeda TA, Pawelec B, Obeso-Estrella R, Díaz de León JN, Fuentes S, Alonso-Núñez G, et al. Competitive HDS and HDN reactions over NiMoS/HMS-Al catalysts: diminishing of the inhibition of HDS reaction by support modification with P. Appl Catal B Environ 2016;180:569–79. https://doi.org/10.1016/j.apcatb.2015.07.013.
[52] To MH, Uisan K, Ok YS, Pleissner D, Lin CSK. Recent trends in green and sustainable chemistry: rethinking textile waste in a circular economy. Curr Opin Green Sustain Chem 2019;20:1–10. https://doi.org/10.1016/j.cogsc.2019.06.002.
[53] Safronov SP, Nagrimanov RN, Samatov AA, Emel'yanenko VN, Zaitsau DH, Pimerzin AA, et al. Benchmark properties of pyrazole derivatives as a potential liquid organic hydrogen carrier: evaluation of thermochemical data with complementary experimental and computational methods. J Chem Thermodyn 2019;128:173–86. https://doi.org/10.1016/j.jct.2018.07.020.
[54] Wechsler D, Cui Y, Dean D, Davis B, Jessop PG. Production of H2 from combined endothermic and exothermic hydrogen carriers. J Am Chem Soc 2008;130:17195–203. https://doi.org/10.1021/ja806721s.
[55] Shuang H, Chen H, Wu F, Li J, Cheng C, Li H, et al. Catalytic dehydrogenation of hydrogen-rich liquid organic hydrogen carriers by palladium oxide supported on activated carbon. Fuel 2020;275:117896. https://doi.org/10.1016/j.fuel.2020.117896.
[56] Santos AFLOM, Gomes JRB, Ribeiro-da-Silva Ma V. 2- and 3-acetylpyrroles : a combined calorimetric and computational study. 2009. https://doi.org/10.1021/jp810407m. 3630–8.
[57] Frisch MJ, Trucks GW, Schlegel HB, Scuseria GE, Robb MA, Cheeseman JR, et al. Gaussian 16 rev. A.03. 2016. Wallingford,CT.
[58] Zhao Y, Truhlar DG. Density functional theory for reaction energies: test of meta and hybrid meta functionals, range-separated functionals, and other high-performance functionals. J Chem Theor Comput 2011;7:669–76. https://doi.org/10.1021/ct1006604.
[59] Verma P, Truhlar DG. Status and challenges of density functional theory. Trends Chem 2020;2:302–18. https://doi.org/10.1016/j.trechm.2020.02.005.
[60] Advanced Search n.d. accessed, https://www.sigmaaldrich.com/catalog/AdvancedSearchPage.do. [Accessed 27 November 2020].
[61] ChemSpider | Search and share chemistry n.d. accessed, http://www.chemspider.com/. [Accessed 1 February 2021].
[62] CompTox chemicals dashboard n.d. accessed, https://comptox.epa.gov/dashboard/predictions/index. [Accessed 2 February 2021].
[63] Zhao Y, Truhlar DG. Design of density functionals that are broadly accurate for thermochemistry, thermochemical kinetics, and nonbonded interactions. J Phys Chem 2005;109:5656–67. https://doi.org/10.1021/jp050536c.
[64] Chai J Da, Head-Gordon M. Long-range corrected hybrid density functionals with damped atom-atom dispersion corrections. Phys Chem Chem Phys 2008;10:6615–20. https://doi.org/10.1039/b810189b.
[65] Mardirossian N, Head-Gordon M ωb97X-V. A 10-parameter, range-separated hybrid, generalized gradient approximation density functional with nonlocal correlation, designed by a survival-of-the-fittest strategy. Phys Chem Chem Phys 2014;16:9904–24. https://doi.org/10.1039/c3cp54374a.
[66] Kosar N, Mahmood T, Ayub K. Role of dispersion corrected hybrid GGA class in accurately calculating the bond dissociation energy of carbon halogen bond: a benchmark study. J Mol Struct 2017;1150:447–58. https://doi.org/10.1016/j.molstruc.2017.08.104.
[67] Peverati R, Truhlar DG. Screened-exchange density functionals with broad accuracy for chemistry and solid-state physics. Phys Chem Chem Phys 2012;14:16187–91. https://doi.org/10.1039/c2cp42576a.
[68] Nishioka M, Lee ML, Castle RN. Sulphur heterocycles in coal-derived products. Relation between structure and

Please cite this article as: Izquierdo R et al., Substituted heterocycles as new candidates for liquid organic hydrogen carriers: *In silico* design from DFT calculations, International Journal of Hydrogen Energy, https://doi.org/10.1016/j.ijhydene.2021.02.201

abundance. Fuel 1986;65:390–6. https://doi.org/10.1016/0016-2361(86)90301-7.
[69] Trofimov BA, Nedolya NA. Pyrroles and their benzo derivatives: reactivity. Compr. Heterocycl. Chem. III. Elsevier; 2008. p. 45–268. https://doi.org/10.1016/B978-008044992-0.00302-3.
[70] Li B, Lin H, Huang L, Jiang H. Pyrroles and their benzo derivatives: synthesis. Ref. Modul. Chem. Mol. Sci. Chem. Eng.. Elsevier; 2020. https://doi.org/10.1016/B978-0-12-409547-2.14911-X.
[71] Korostova SE, Mikhaleva AI, Trofimov BA. Bipyrroles, furyl- and thienylpyrroles. Usp Khim 1999;68:528–31. https://doi.org/10.1070/rc1999v068n06abeh000451.
[72] Joule JA. Five-membered ring systems: thiophenes and selenium/tellurium analogs and benzo analogs. Prog Heterocycl Chem 2020;31:177–222. https://doi.org/10.1016/B978-0-12-819962-6.00005-1. Elsevier Ltd.
[73] Vivancos Á, Beller M, Albrecht M. NHC-based iridium catalysts for hydrogenation and dehydrogenation of N-heteroarenes in water under mild conditions. ACS Catal 2018;8:17–21. https://doi.org/10.1021/acscatal.7b03547.
[74] Liu W, Jiang Y, Dostert KH, O'Brien CP, Riedel W, Savara A, et al. Catalysis beyond frontier molecular orbitals: selectivity in partial hydrogenation of multi-unsaturated hydrocarbons on metal catalysts. Sci Adv 2017;3. https://doi.org/10.1126/sciadv.1700939.
[75] Senthamaraikannan TG, Min Y, Lee JH, Song TY, Lim DH. Dehydrogenation of ethylene diamine monoborane adducts and their cyclic products (monomers, dimers, and trimers): potential liquid organic hydrogen carriers. Int J Hydrogen Energy 2021;46:7336–50. https://doi.org/10.1016/j.ijhydene.2020.11.234.

Please cite this article as: Izquierdo R et al., Substituted heterocycles as new candidates for liquid organic hydrogen carriers: *In silico* design from DFT calculations, International Journal of Hydrogen Energy, https://doi.org/10.1016/j.ijhydene.2021.02.201